NeuroResource

Neuron

Chemoconnectomics: Mapping Chemical Transmission in *Drosophila*

Highlights

- The authors propose a new concept of the chemoconnectome (CCT) for chemical transmission
- Chemoconnectomics with genetic tools is a new approach for neural mapping
- CCT research in *Drosophila* will stimulate CCT studies in higher animals

Authors

Bowen Deng, Qi Li, Xinxing Liu, ..., Wenxia Zhang, Juan Huang, Yi Rao

Correspondence

yrao@pku.edu.cn

In Brief

Deng et al. propose the concept of the chemoconnectome (CCT) as the entirety of all neurotransmitters, neuromodulators, neuropeptides, and their receptors and the approach of chemoconnectomics to trace neural circuitry anatomically and functionally.

Deng et al., 2019, Neuron *101*, 1–18
March 6, 2019
https://doi.org/10.1016/j.neuron.2019.01.045

CellPress

Please cite this article in press as: Deng et al., Chemoconnectomics: Mapping Chemical Transmission in *Drosophila*, Neuron (2019), https://doi.org/10.1016/j.neuron.2019.01.045

Neuron
NeuroResource

Chemoconnectomics: Mapping Chemical Transmission in *Drosophila*

Bowen Deng,[1,3] Qi Li,[1,3] Xinxing Liu,[1,3] Yue Cao,[1,3] Bingfeng Li,[1] Yongjun Qian,[1] Rui Xu,[2] Renbo Mao,[1] Enxing Zhou,[1] Wenxia Zhang,[1] Juan Huang,[2] and Yi Rao[1,4,*]

[1]Peking-Tsinghua Center for Life Sciences, PKU-IDG/McGovern Institute for Brain Research, Advanced Innovation Center for Genomics, Peking University School of Life Sciences, Chinese Institute for Brain Research, Beijing, Zhongguangchun Life Sciences Park, Beijing, China
[2]School of Basic Medical Sciences, Nanjing Medical University, Nanjing, China
[3]These authors contributed equally
[4]Lead Contact
*Correspondence: yrao@pku.edu.cn
https://doi.org/10.1016/j.neuron.2019.01.045

SUMMARY

We define the chemoconnectome (CCT) as the entire set of neurotransmitters, neuromodulators, neuropeptides, and their receptors underlying chemotransmission in an animal. We have generated knockout lines of *Drosophila* CCT genes for functional investigations and knockin lines containing Gal4 and other tools for examining gene expression and manipulating neuronal activities, with a versatile platform allowing genetic intersections and logic gates. CCT reveals the coexistence of specific transmitters but mutual exclusion of the major inhibitory and excitatory transmitters in the same neurons. One neuropeptide and five receptors were detected in glia, with octopamine β2 receptor functioning in glia. A pilot screen implicated 41 genes in sleep regulation, with the dopamine receptor Dop2R functioning in neurons expressing the peptides Dilp2 and SIFa. Thus, CCT is a novel concept, chemoconnectomics a new approach, and CCT tool lines a powerful resource for systematic investigations of chemical-transmission-mediated neural signaling circuits underlying behavior and cognition.

INTRODUCTION

The connectome is the entire set of neural connections within the nervous system and its targets in an animal (Sporns et al., 2005; Bargmann and Marder, 2013). The connectome can be studied at multiple levels; electron microscopy (EM) can visualize the hard wiring of every neuron (Kasthuri et al., 2015; Morgan et al., 2016; White et al., 1986; Zheng et al., 2018), while magnetic resonance imaging (MRI) can visualize general patterns of connectivity (Glasser et al., 2016). Between them is the mesoconnectome, which can be studied by viral injections of markers or manipulators driven by cell-type-specific promoters (Beier et al., 2015; Lerner et al., 2016; Luo et al., 2018; Oh et al., 2014a; Watabe-Uchida et al., 2012). Each approach has advantages and disadvantages. EM and MRI lack molecular resolution and cannot manipulate molecular or cellular functions. While viral injections can overcome many of the above problems, it is unclear how many viral injections (at how many locations of the nervous system with how many promoters) are necessary. Thus, with the exception of the worm *Caenorhabditis elegans*, which contains only 302 neurons (White et al., 1986), the connectomes of larger nervous systems remain unclear.

Each neuron is endowed chemically with the presence of small-molecule transmitters, modulators, and peptides (Cooper et al., 2003). Here, we define the chemoconnectome (CCT) as all neurotransmitters, modulators, neuropeptides, and their receptors in an animal. Signaling between neurons and their target cells is mediated by chemical and electric transmission, with chemical transmission as the predominant mode (Loewi, 1921). Typically, a presynaptic neuron synthesizes and stores neurotransmitters in synaptic vesicles and, upon stimulation, releases transmitters and modulators, which diffuse across the synaptic cleft and act on receptors located on the cytoplasmic membrane of post-synaptic neurons or other target cells. Classical experiments have uncovered neurotransmitters, including acetylcholine (ACh) (Hunt and Taveau, 1906; Dale, 1914; Dale and Feldberg, 1934), noradrenaline (NA) (Oliver and Schäfer, 1895; Takamine, 1901, 1902; Elliot, 1904; Von Euler, 1946), histamine (Barger and Dale, 1910), 5-hydroxytryptophan (5-HT) (Erspamer and Vialli, 1937; Rapport et al., 1948), dopamine (DA) (Montagu, 1957; Carlsson et al., 1958), glutamate (Glu) (Curtis et al., 1959), and γ-aminobutyric acid (GABA) (Roberts and Frankel, 1950; Udenfriend, 1950). Peptides have been discovered in the nervous system to serve as either transmitters or modulators (Von Euler and Gaddum, 1931; Hughes et al., 1975). Neurotransmitters and neuromodulators and neuropeptides act on receptors, of which some are ionotropic receptors and some are G-protein-coupled receptors (GPCRs). Abnormalities of neurotransmission have been implicated in multiple diseases, with ~34% of US Food and Drug Administration (FDA)-approved drugs targeting GPCRs (Hauser et al., 2017). Thus, investigations of transmitters and receptors may provide insights in understanding human diseases and developing new drugs.

In *Drosophila*, we and others have studied the roles of transmitters and receptors in a variety of behaviors (Zhou et al., 2008, 2012; Liu et al., 2011; Qian et al., 2017), usually one or a

few neurotransmitters at a time. The CCT is a systematic approach that requires us to generate knockout (KO) and knockin (KI) lines targeting all known small-molecule transmitters, modulators, neuropeptides, and their receptors. 193 genes related to synthetases or transporters for transmitters, modulators, neuropeptides, their receptors, and non-olfactory orphan GPCRs were selected. KO lines for CCT enable studies of loss-of-function phenotypes of each transmitter or receptor. KI lines for CCT enable visualization of neurons expressing each transmitter or receptor. We have carried out proof-of-principle experiments to show that chemoconnectomics provides a powerful approach to study neural signaling. By highlighting the neurochemical features of transmitters, modulators, and neuropeptides, the CCT approach aims at, and its associated resources provide tools for, investigating functions of transmitters, modulators, neuropeptides, their receptors, and neurons expressing them. The KO lines allow examination of the functional involvement of each transmitter/modulator/neuropeptide and receptor in behaviors, while the KI lines allow examination of the expression patterns of transmitters, modulators, neuropeptides, and their receptors. Together, they facilitate the dissection of neurochemically defined circuitry. Chemoconnectomics complements, and has advantages over, macro-, meso-, and microconnectomics for studying neural circuitry and conventional mutagenesis for studying genes involved behavior. It has not escaped our notice that CCT should be generated in mammals to facilitate delineation of neural circuits underlying behaviors and cognition.

RESULTS

Genetic Targeting of Neurotransmitters, Modulators, Neuropeptides, and Their Receptors

While neuropeptides can be targeted straightforwardly through their corresponding genes (Hewes and Taghert, 2001), small-molecule transmitters and modulators can be targeted indirectly by specific enzymes or vesicular or cell surface transporters (Figure 1A). Receptors for all small-molecule transmitters and modulators and, for some neuropeptides, together with orphan GPCRs were targeted. In *Drosophila*, we have chosen 193 genes, including those encoding synthesizing enzymes for 10 of 11 small-molecule transmitters/modulators, those encoding 6 transporters, 40 neuropeptides, 32 ionotropic receptors, 59 metabotropic receptors, and 44 orphan GPCRs (Tables S1 and S2). Two of the small-molecule transmitters, Glu and glycine, were targeted not by synthesizing enzyme but by transporters (VGluT and GlyT).

We used the CRISPR-Cas9 system to generate KO lines (Ran et al., 2013) (Figure 1B) with an attP docking site introduced to generate an attP-KO line, which provides a versatile platform for further genetic modifications, including KI and protein trapping by phiC31-mediated gene integration (Groth et al., 2004) (Figure 1C; Table S2).

We generated KI lines by fusing the Gal4 protein to the C terminus of a protein of interest with the stop codon for that protein removed and replaced with T2A. Gene expression could thus be visualized after crossing a Gal4 KI line to the *UAS-mCD8::GFP* reporter line (Figure 1D). Of the 128 gene KI Gal4 lines in which we have examined expression so far, 106 were detected in the brain. We generated KI lines for different isoforms if they exist for a single gene (Figure S1). As shown for the neuropeptide ion transport protein (ITP) and three GPCRs (Dh31-R, CCHa2-R, and DopR2), isoforms had distinct patterns.

Our basic constructs allow flexibility and versatile applications, facilitating the generation of Flp, Lex A, and p65AD (Figure 4A) lines, as well as superfold GFP (sfGFP) lines for protein localization (Pédelacq et al., 2006). With sfGFP fused to Dop1R1, a DA receptor (DR) in *Dop1R1::sfGFP*, we detected its expression in the mushroom bodies (MBs) (Figures 1F and 1G). Similarly, we detected MB expression of a 5-HT receptor (in *5HT1A::sfGFP*) (Figures 1H and 1I). We compared Gal4 and LexA KI lines for 10 genes; Gal4 and LexA KIs for the same gene usually had very similar patterns (those shown in Figures 1D and 1E are for *CCHa2*), although the patterns observed for Gal4 and LexA were quite different for *CCAPR* (Figure S2).

Neuronal Distribution of CCT Genes

Our KI lines make it possible to examine the distribution of neurons expressing neuropeptides as well as those for synthetases or transporters of small-molecule transmitters and receptors. 11 small molecules (ACh, GABA, Glu, Gly, DA, 5-HT, octopamine (OA), histamine (HA), tyramine (TA), adenosine (Ado), and D-serine) have been reported in *Drosophila* (Dolezelova et al., 2007; Kong et al., 2010; Yamazaki et al., 2014).

We have generated the following KI Gal4 lines to cover small-molecule transmitters: ACh by genetic tagging of choline acetyltransferase (*ChAT*) (Greenspan, 1980; Itoh et al., 1986; Kitamoto et al., 1992), GABA by tagging glutamic acid decarboxylase (*GAD1*) (Jackson et al., 1990) and the vesicular GABA transporter (*VGAT*) (Fei et al., 2010), glycine by tagging glycine transporter (*GlyT*) (Frenkel et al., 2017), Glu by tagging the vesicular Glu transporter (*VGluT*) (Daniels et al., 2004), DA by tagging tyrosine hydroxylase (*TH*) (Budnik and White, 1988; Neckameyer and Quinn, 1989; Mao and Davis, 2009) and the DA transporter (*DAT*) (Pörzgen et al., 2001), 5-HT by tagging tryptophan hydroxylase (*TrH*) (Neckameyer and White, 1992) and the cytoplasmic 5-HT transporter (*SerT*) (Corey et al., 1994; Demchyshyn et al., 1994), OA by tagging the TA β hydroxylase (*TβH*) (Monastirioti et al., 1996), and HA by tagging the histidine decarboxylase (*HDC*) (Burg et al., 1993). TA cannot be specifically tagged, but TDC2-Gal4 covers the combined pattern of TA and OA (Cole et al., 2005). We have also generated LexA KI lines for all of these genes and Flp KI lines for *ChAT*, *VGluT*, *GAD1*, *TrH*, and *TH*.

Neurons expressing these genes were visualized after the Gal4 KI lines were crossed to the *UAS-mCD8::GFP* reporter line (Figure 2). Distinct patterns have been observed for *ChAT* (Figure 2A), *VGluT* (Figure 2B), *VGAT* (Figure 2C), *HDC* (Figure 2D), *DAT* (Figure 2E), *TH* (Figure 2F), *SerT* (Figure 2G), and *TβH* (Figure 2H). The pattern of *SerT* is similar to that of *TrH* reported by us recently (Qian et al., 2017).

We generated KO and KI lines targeting the neuropeptide genes known from previous reports and predicted from bioinformatics (Broeck, 2001; Hewes and Taghert, 2001; Nässel and Winther, 2010). Expression patterns of neuropeptides are

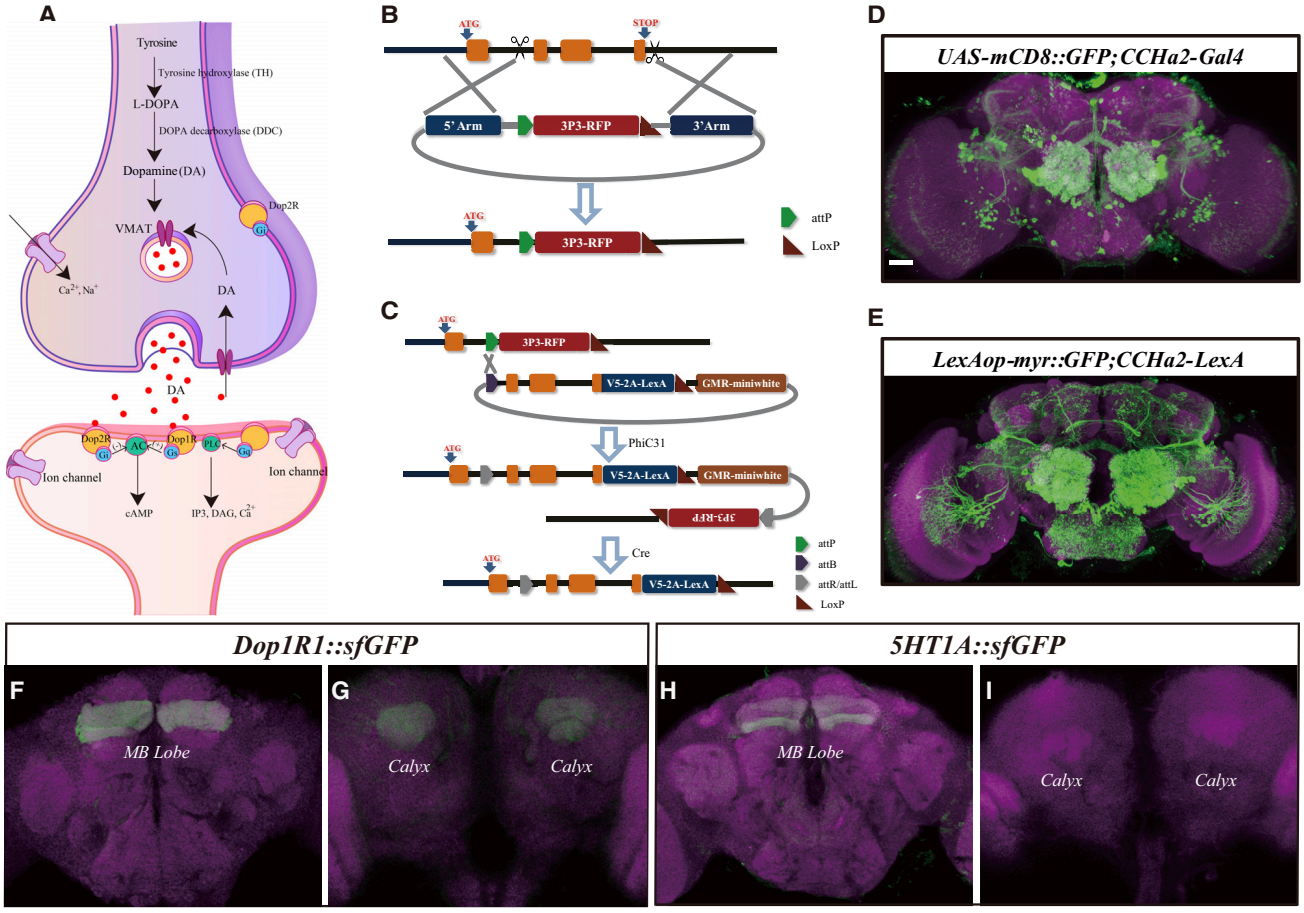

Figure 1. KO and KI Lines in *Drosophila* CCT

(A) A dopaminergic synapse: DA synthesis and transport and DRs.

(B) Homologous-recombination-mediated gene targeting. To generate a KO, most of the exons were replaced by the 3P3-RFP cassette through homologous recombination, and CRISPR-Cas9 was used to increase the targeting efficiency. In addition, an attP site before the 3P3-RFP cassette was inserted into the non-transcriptional region to allow for further modifications.

(C) Site-specific integration system mediated KI. The KI cassette including the genomic region deleted in the KO lines and KI elements such as the Gal4 or LexA coding sequence were introduced through PhiC31-mediated attP/attB recombination. *loxP* sites were also introduced.

(D and E) Expression of *UAS-mCD8-GFP* driven by *CCHa2-Gal4* (D), and of *LexAop-myr::GFP* driven by *CCHa2-LexA* (E). Green, GFP; magenta, nc82. Scale bar, 30 μm.

(F and G) Protein localization revealed by sfGFP fused in-frame to Dop1R1 at MB lobe region (F) and calyx region (G).

(H and I) Protein localization revealed by sfGFP fused in-frame to 5-HT1A receptor at MB lobe region (H) and calyx region (I).

Green, sfGFP; magenta; nc82. Scale bar, 30 μm.

shown in Figures 2 and S1–S4. Neuropeptides were usually detected in limited regions (Figures 2I–2T), whereas their receptors were detected in broader patterns (Figures 2Y–2Bb and S3). Neurons expressing *SIFaR*, *CNMaR*, or *NPFR* (Figures 2Y, 2Z, 2Aa, and 2Bb) were more in number and innervated more broadly than neurons expressing *SIFa*, *CNMa*, or *NPF* (Figures 2J, 2M, and 2N).

Two Glu receptors (*GluRIA* and *GluRIB*) were detected in the MBs and antennal lobe (AL), and *GluRIB* was also detected in the supraesophogeal ganglion (SOG) and the visual system (Figures 2U and 2V). There are five genes encoding GABA receptors, two for GABA-A (Ffrench-Constant et al., 1991; Henderson et al., 1993) and three for GABA-B (Mezler et al., 2001). *GABA-B-R1* was found in the AL, visual system, MBs and ellipsoid body (EB); *GABA-B-R3* was found in the EB, but not in the MB (Figures 2W and 2X).

Glial Expression of CCT Genes

Genes for small-molecule transmitters, modulators, and neuropeptides were detected in neurons (Figures 1D–1H and 2). Are any of these genes expressed in glial cells?

So far, we have not detected the expression of small-molecule transmitters or modulators in glia. However, we have detected the expression of one neuropeptide and five receptors in glial cells. The expression of the RD isoform of the ITP neuropeptide gene was found in glia and neurons (Figure 3A). The RC isoform of the receptor for Dh31 neuropeptide was also detected in glia and neurons (Figure 3B). An isoform of the

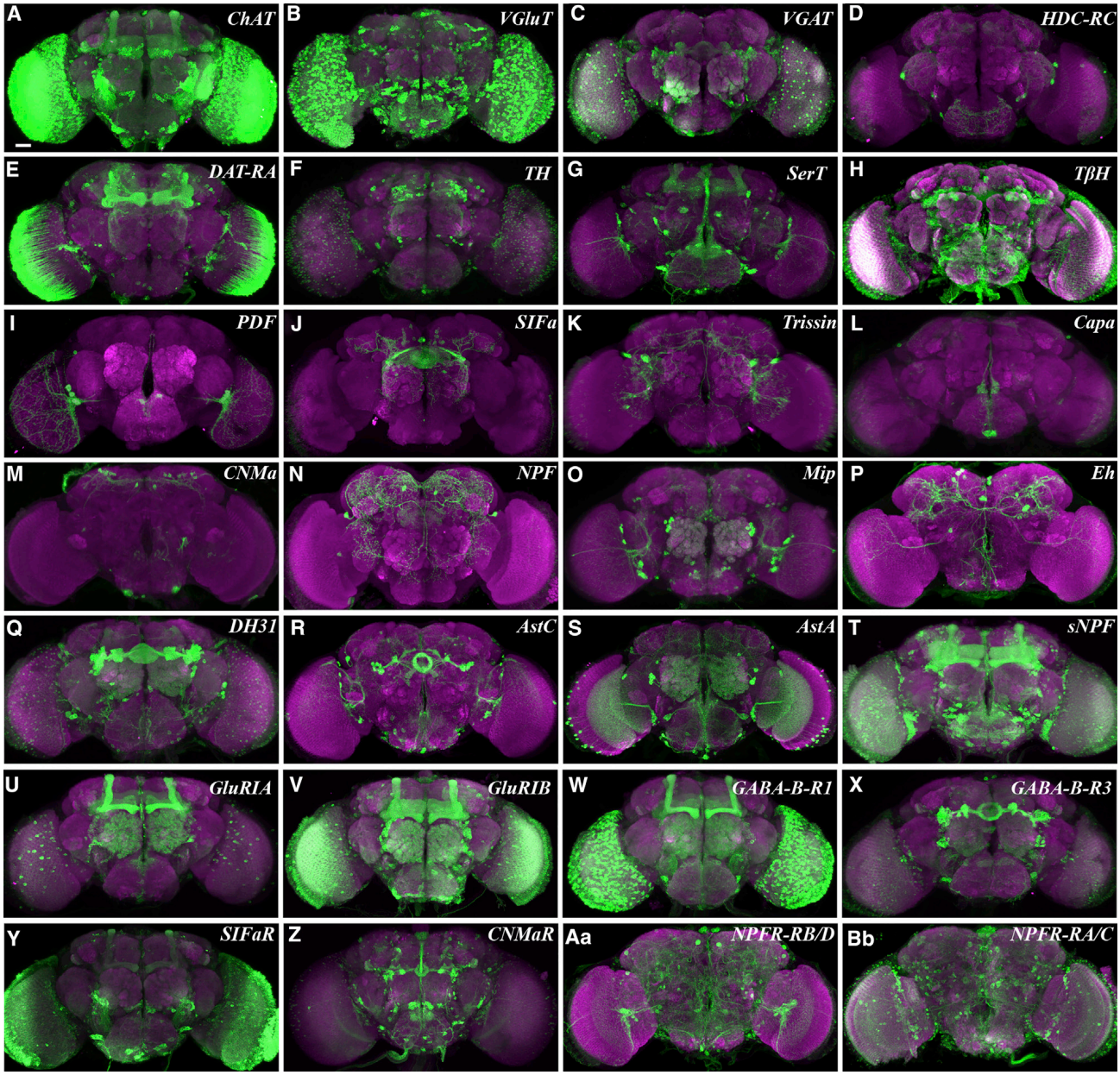

Figure 2. Distribution of Neurons Expressing CCT Genes Revealed by KI Lines

(A–H) Expression patterns of genes encoding ChAT, a marker for Ach (A), VGluT for Glu (B), VGAT for GABA (C), HDC-RC for HA (D), DAT-RA for DA (E), TH for DA (F), SerT for 5-HT (G), and TβH for OA (H). The HDC-RA/B isoform was not detected in the brain.

(I–T) Expression patterns of neuropeptides in the brain for PDF (I), SIFa (J), Trissin (K), Capa (L), CNMa (M), NPF (N), Mip (O), Eh (P), DH31 (Q), AstC (R), AstA (S), and sNPF (T).

(U–X) Expression patterns of gene encoding GluR1A (U) and GluR1B (V), GABA-B-R1 (W), and GABA-B-R3 (X).

(Y–Bb) Expression patterns of neuropeptide receptors neurons in the brain: SIFaR (Y), CNMaR (Z), NPFR-RB/D (Aa) isoform, and NPFR-RA/C isoform (Bb).

Dop1R1 receptor was found in glia and neurons (Figure 3C). With the help of multiple glial Gal4 lines, we detected *ITP-RD* in perineurial, cortical astrocyte-like, and ensheathing glia, *Dh31R-RC* in subperineurial and cortical glia, and *Dop1R1-RB/C* in cortical and ensheathing glia (Figure S4). The Ado receptor (AdoR) (Figures S3D and S5) and Lk receptor (LkR) (unpublished data) were also detected in glia. AdoR inhibits male-male aggression (Figure S5), though we have not determined whether it functions in neurons or glia.

The octopamine β2 receptor (Octβ2R) was detected in both neurons and glia (Figures 3E–3J). Nuclear GFP expression driven by *Octβ2R-Gal4* overlapped with immunostaining by the anti-Repo antibody, a pan-glial marker (Figures 3E–3G). Overlap was also detected between *Octβ2R* and immunostaining of the

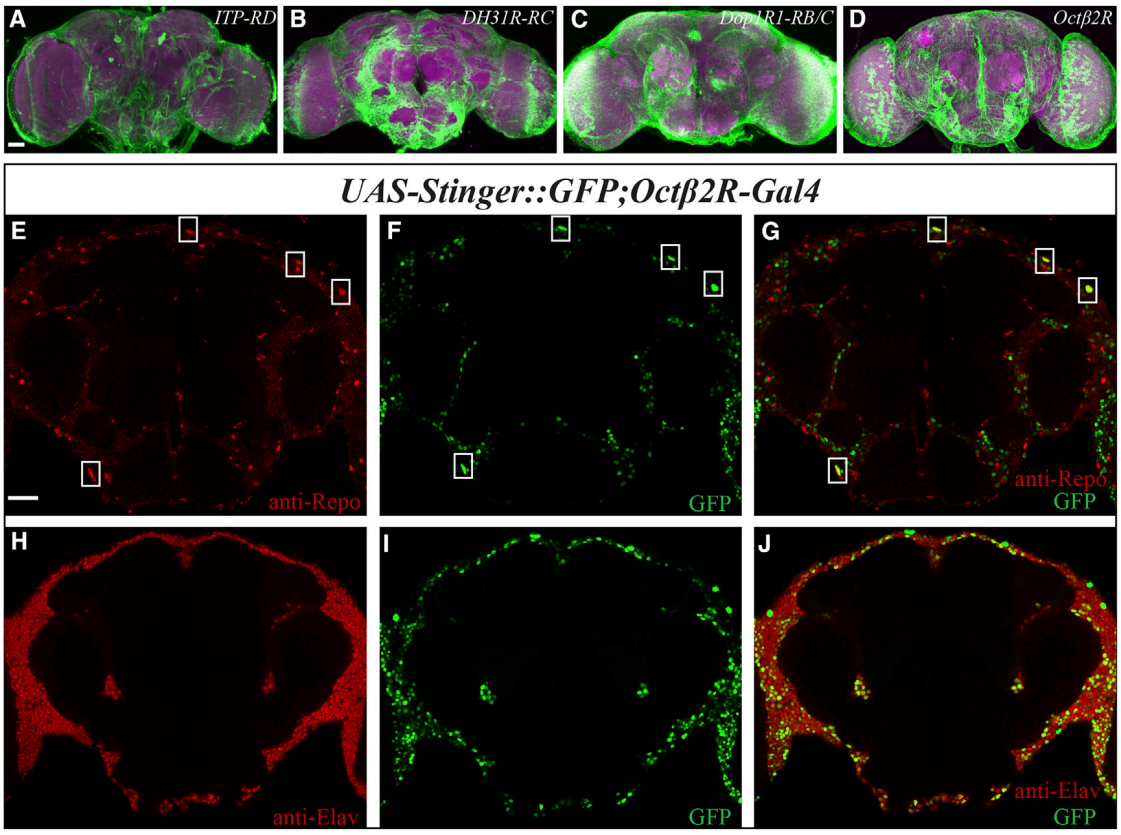

Figure 3. Analysis of Glial Expression of CCT Genes

(A–D) Glia expression of neuropeptide or receptor isoform after crossing isoform-specific KI Gal4 to *UAS-mCD8::GFP*: *ITP-RD* (A), *DH31-RC* (B), Dop1R1RB/C (C), and *Octβ2R* (D).

(E–G) Octβ2R-positive nuclei were revealed by *UAS-Stinger::GFP* driven by *Octβ2R-Gal4*. Overlap of Octβ2R gene expression with immunostaining by the anti-Repo antibody was detected (G). The anti-Repo channel and GFP channel are separately shown (E) and (F).

(H–J) Overlap of Octβ2R expression with immunostaining by the anti-Elav antibody was detected (J). The anti-Elav channel and GFP channel are separately shown (I) and (J).

anti-Elav antibody, a pan-neuronal marker (Figures 3H–3J). Evidence for Octβ2R function in glia will be presented below (Figures 6and S7).

Expression of Transmitters and Receptors in Dopaminergic Neurons

Henry Dale proposed that the same transmitter would be released from different terminals of the same neuron (Dale, 1935). This was generalized by John Eccles as "Dale's principle" that each neuron makes only one transmitter (Eccles et al., 1954; Eccles, 1976). This simple version has been shown to be incorrect, because multiple transmitters have been found to coexist in the same neuron and co-transmit (Lundberg, 1996; Nicoll and Malenka, 1998; Granger et al., 2017). However, it is unclear which transmitters coexist with other transmitters.

Using DA as a test case in *Drosophila*, we used an intersectional strategy based on the split-LexA system (Luan et al., 2006; Pfeiffer et al., 2010; Ting et al., 2011) (Figure 4A) to investigate whether other neurotransmitters and neuropeptides were expressed in dopaminergic neurons. The transcriptional activation domain (p65AD) of the human p65 protein was inserted in the C terminus of the TH protein, which could activate the expression of a membrane-targeted GFP (myr::GFP) only when the DNA-binding domain (DBD) of LexA interacted with the LexA operator upstream of GFP; because LexA DBD was downstream of the upstream activation sequence (UAS) for Gal4, GFP would only be expressed when the Gal4 fused to gene X is expressed. Here, X is a CCT gene. We have generated p65AD lines for *ChAT*, *VGluT*, *GAD1*, *TrH*, and *TH*.

A line expressing TH-p65AD was crossed to 24 KI Gal4 lines for ligands (including small-molecule neurotransmitters, modulators, and neuropeptides) and to 61 KI Gal4 lines for receptors. Receptor KI Gal4 lines with expression in brain were selected for the intersection experiments. We observed positive intersectional signals from 16 of the 24 ligand Gal4 lines and all 61 receptor Gal4 lines (Figures 4B–4K). All four DRs were observed in dopaminergic neurons (Figures 4I–4K and S5A–S5P; data not shown), suggesting their possible functions as autoreceptors in different neurons.

We compared intersection results with immunostaining with an anti-TH antibody (Figure S6) and found that more neurons were detected by the intersection strategy than those detected

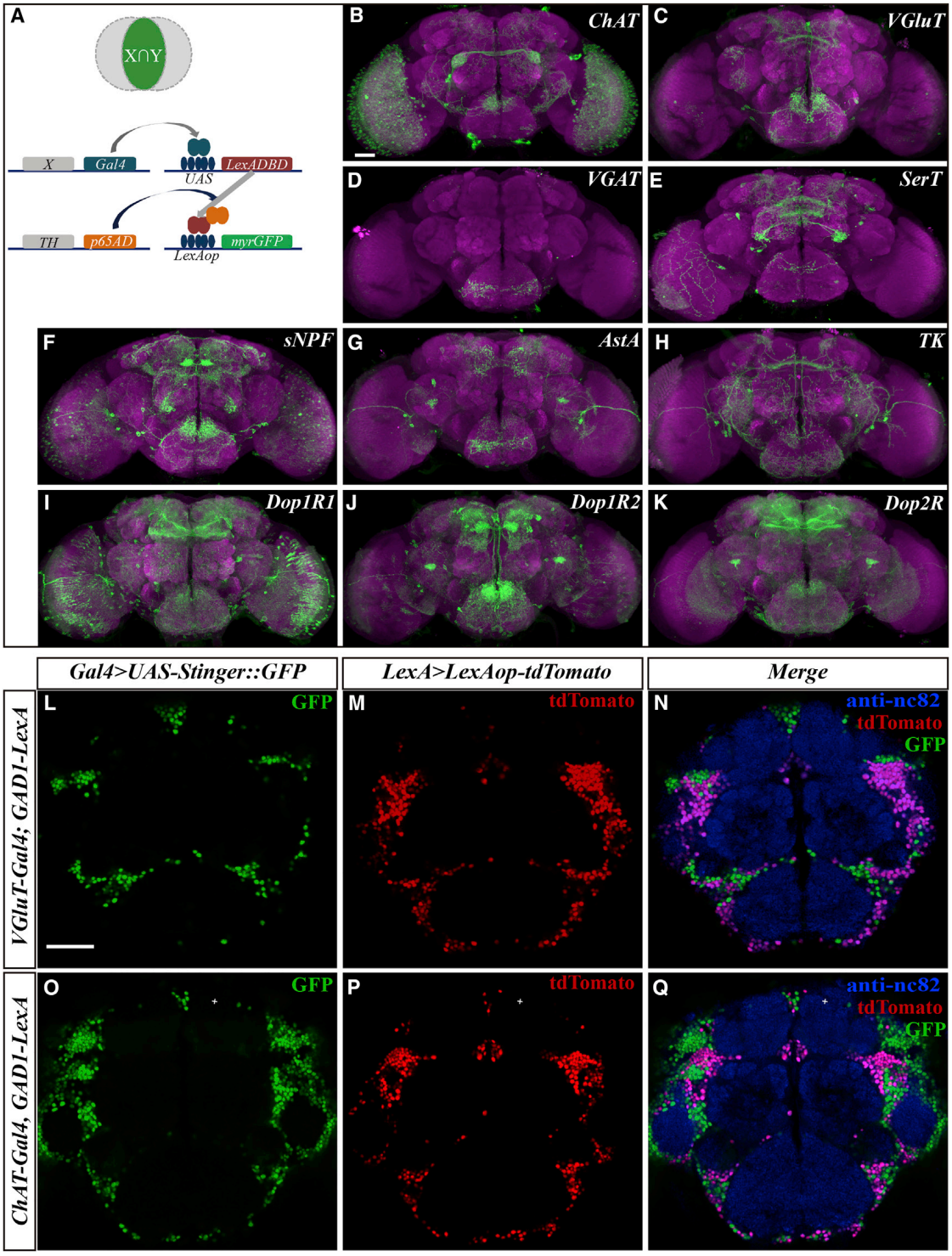

Figure 4. Expression Patterns of Two Transmitters

(A–K) Intersectional analysis with split LexA (see text for detailed explanation). TH-positive neurons intersected with *ChAT* (B), *VGluT* (C), *VGAT* (D), *SerT* (E), *sNPF* (F), *AstA* (G), and *TK* (H). Expression of DRs in TH-positive neurons is shown for *Dop1R1* (I), *Dop1R2* (J), and *Dop2R* (K). Green, GFP; magenta, nc82. Scale bars, 30 μm.

(L–N) *VGluT*-expressing neurons were labeled by nuclearly localized GFP in *UAS-stinger::GFP* driven by *vGlut-Gal4* (L) and GAD1-expressing neurons by tdTomato in *LexAop-tdTomato* driven by *GAD1-LexA* (M). No overlap was detected between them (N). Blue, nc82, an antibody recognizing all neuronal nuclei.

(O–Q) *ChAT*-expressing neurons were labeled by nuclearly localized GFP in *UAS-stinger::GFP* driven by *ChAT-Gal4* (O) and GAD1-expressing neurons by tdTomato in *LexAop-tdTomato* driven by *GAD1-LexA* (P). No overlap was detected between them (Q). Blue, nc82.

by the anit-TH antibody, especially in posterior brain regions (Figures S6A–S6P). For example, most of PAM TH$^+$ neurons expressed Dop2R (only 5 PAM TH$^+$ neurons negative for Dop2R) (Figure S6G), whereas only ~10 PAM TH$^+$ neurons expressed Dop1R2 (Figure S6O), which was consistent with the intersection results (Figures S6A and S6I). In the lobula, where the TH antibody signal could not be detected, intersectional signals were strong for Dop2R (Figure S6B). However, the intersectional signal at the lobula was quite similar to that in *TH-KI-Gal4>UAS-GFP* (Figure S6R). Because the Gal4/UAS and LexA/LexAop systems could amplify expression signals, the intersection strategy and *TH-KI-Gal4* could reveal neurons that were otherwise weak in TH expression (Figures S6Q–S6R1).

We also compared our intersection results with previous studies from RNA sequencing (RNA-seq) of either isolated DA neurons (Abruzzi et al., 2017) or single cells from the midbrain (Croset et al., 2018). Of the 85 genes analyzed in intersections, expression of all 16 for small-molecule transmitters and peptides positive for the intersectional signal with *TH-p65AD* was detected in DA neurons by both RNA-seq studies. However, several peptides negative in our intersections, such as prothoracicotropic hormone (Ptth) and Trissin, were detected by RNA-seq. One peptide, Lk, was detected in DA neurons by Abruzzi et al., but not by Croset et al. Of the 61 genes for receptors positive in intersections, Abruzzi et al. detected 45 in DA neurons, while Croset et al. detected all of them in at least one DA neuron. In addition, although most of the receptor genes were expressed at low levels (Abruzzi et al., 2017), they could be expressed broadly in DA neurons (Croset et al., 2018). We analyzed the single-cell sequencing data from 644 TH$^+$ neurons (Croset et al., 2018) and found expression of 29 out of 31 genes for ion channels in DA neurons. On average, an ion channel gene was expressed in 22.3% of DA neurons. For GPCRs, 86 out of 98 genes could be detected in DA neurons, and on average, a GPCR was expressed in 7% of DA neurons. 29 out of 35 peptide genes were expressed in DA neurons, however, on average, a peptide was expressed in 3.4% of DA neurons. The broad expression of ion channels and sparse expression of peptide genes in DA neurons were consistent with our intersectional results. However, our intersection results suggested that both the ion channels and GPCRs were expressed more broadly than single-cell sequencing results. At this point, it cannot be distinguished whether single-cell sequencing was not sensitive to the capture of low-expression genes or that intersection is oversensitive to the detection of co-expression, including transient ones.

No Expression of *GAD1* in *VGluT*- or *ChAT*-Positive Neurons

In mammals, the excitatory transmitter Glu and the inhibitory transmitter GABA have been thought to be co-transmitters (Trudeau, 2004; El Mestikawy et al., 2011; Granger et al., 2017), as evidenced by co-expression of VGluT1 and GAD65 (Kao et al., 2004; Herzog et al., 2004a, 2004b) or VGluT and VGAT in the same neurons (Ottem et al., 2004; Fattorini et al., 2009). VGluT and VGAT were detected in different (Boulland et al., 2009) or the same synaptic vesicles (Zander et al., 2010).

In *Drosophila*, Glu and ACh are the major excitatory transmitters and GABA is the major inhibitory transmitter. To investigate the relationship between excitatory and inhibitory transmitters in the *Drosophila* brain, we used two different binary expression systems, Gal4/UAS and LexA/LexAop, to label excitatory and inhibitory neurons simultaneously. GABAergic neurons were shown as stinger::GFP driven by GAD1-LexA, and glutamatergic neurons and cholinergic neurons were shown as tdTomato driven by either VGluT-Gal4 or ChAT-Gal4. No overlap was detected between GFP and tdTomato signals when GFP was driven by VGluT and tdTomato by GAD1 (Figures 4L–4N) or when GFP was driven by ChAT and tdTomato by GAD1 (Figures 4O–4Q), indicating that unlike mammals (Granger et al., 2017), GABAergic inhibitory neurons in *Drosophila* do not express either of the excitatory transmitters (Glu or ACh).

Complex Relationship between Genes Encoding Neuropeptides and Neurons Expressing These Genes

Sleep has been studied for nearly two decades in *Drosophila* (Hendricks et al., 2000; Shaw et al., 2000). We used a video-based assay for sleep (Oh et al., 2014b; Qian et al., 2017) to screen 147 KO lines (Figure 5A). Lines with changes of more than 20% were selected for further verification. 41 genes were found to regulate sleep (Table S3), including known regulators of sleep such as *5HT1a* and *Mip* in promoting sleep (Oh et al., 2014b; Qian et al., 2017; Yuan et al., 2006) and *Dop1R1* and *Dop1R2* (Liu et al., 2012; Pimentel et al., 2016; Ueno et al., 2012), as well as newly uncovered genes.

We further used the KI lines to investigate neuronal involvement in sleep by driving NaChBac or Kir2.1 expression (Thum et al., 2006). NaChBac is a voltage-sensitive sodium channel derived from bacteria thath can be used to activate neurons (Luan et al., 2006), while Kir2.1 is a potassium channel that can inactivate neurons (Baines et al., 2001). *UAS-NaChBac* or *UAS-Kir2.1* flies were crossed to Gal4 lines expressing a neuropeptide (Dsk, Tk, or CCHa1) (Figure 5B). Neither activation nor inhibition of Dsk neurons affected sleep (Figure 5B). Inhibiting Tk neurons delayed nighttime sleep latency (Figure 5C), whereas activating Tk neurons significantly increased daytime sleep duration (Figures 5B and 5C). Activating CCHa1 neurons decreased nighttime sleep duration (Figures 5B and 5E), and inhibiting CCHa1 neurons delayed nighttime sleep latency (Figure 5E).

In $Tk^{-/-}$ mutants, daytime and nighttime sleep duration was significantly decreased (Figure 5D; Table S3). Thus, both the *Tk* gene and *Tk*-expressing neurons promote daytime sleep, but the $Tk^{-/-}$ phenotype of nighttime sleep was not observed in *Tk* neuronal inhibition, indicating the presence of other molecules in Tk neurons. Nighttime sleep was decreased in $CCHa1^{-/-}$ mutants (Figure 5F), but CCHa1 neuronal activation decreased sleep (Figure 5E). As shown in other contexts, the consequences of altering activity in a given neuronal cell type may not equate with the consequences of suppressing just one of its secreted factors. Future investigations should examine multiple transmitters and neuropeptides in the same neurons to understand the neural circuitry of behaviors.

OA Regulation of Sleep by Signaling to Both Neuronal and Glial Cells

Our CCT KO screen showed sleep decreases in $Oa2^{-/-}$ and $Oct\beta2R^{-/-}$ mutants (Table S3). They encode receptors for OA,

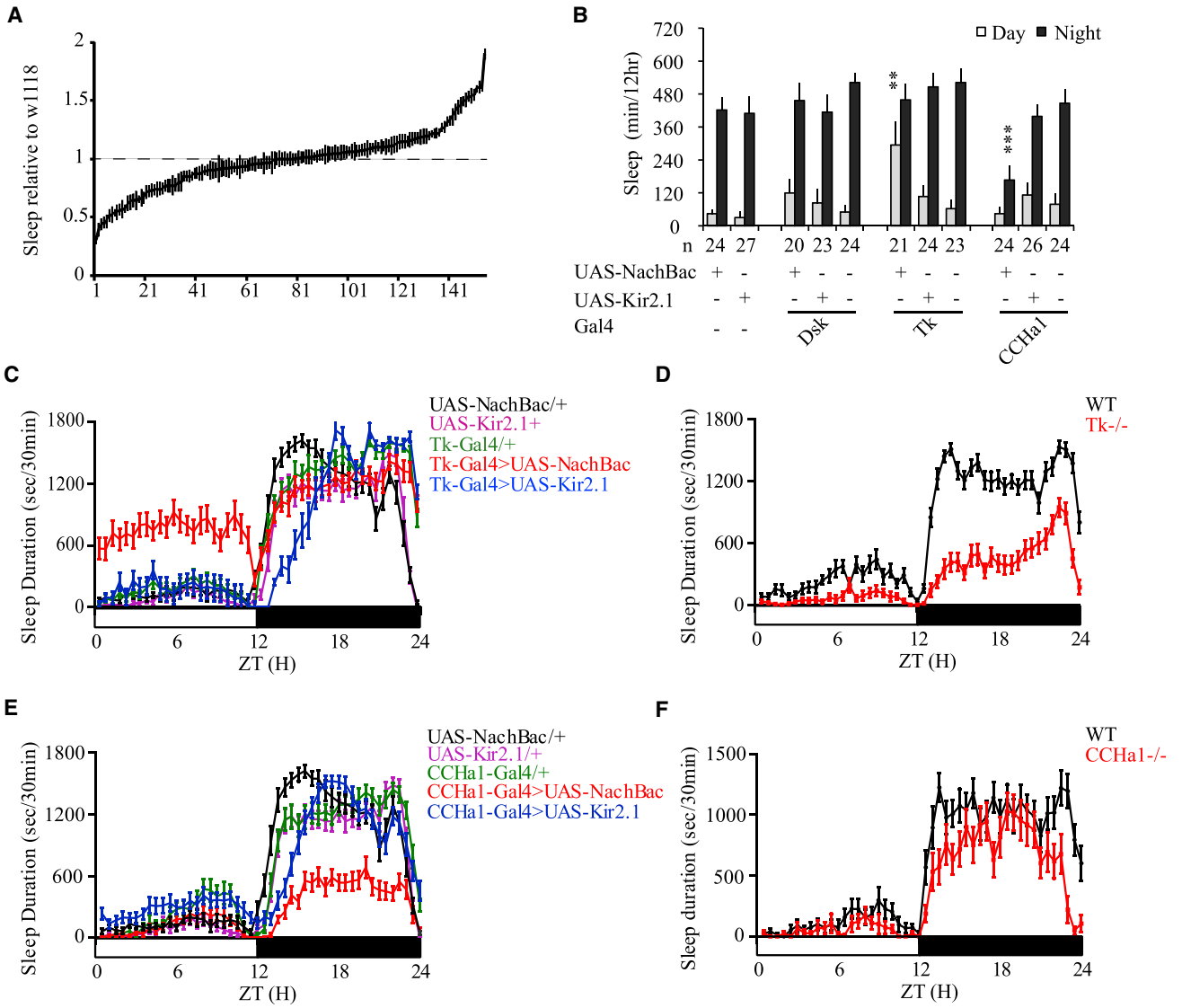

Figure 5. Sleep Analysis of Genetic KOs and Neuronal Manipulations

(A) Results of a pilot screen with 147 KO lines from our CCT showing the total daily amount of sleep relative to the control w1118 (n = 18–30/line). The Mann-Whitney test was used to compare each KO with w1118, and KO lines with significant sleep changes are shown in Table S3. *, **, and *** denote $p < 0.05$, $p < 0.01$, and $p < 0.001$, respectively.

(B) Sleep after activating or inhibiting the activity of neurons expressing neuropeptides (Dsk, Tk, and CCHa1). Numbers below each bar represent the number of flies tested. Mean ± SEM is shown. The Kruskal-Wallis test followed by Dunn's post test was used. *, **, and *** denote $p < 0.05$, $p < 0.01$, and $p < 0.001$, respectively.

(C) Sleep profiles of flies after increasing (NaChBac) or decreasing (Kir2.1) the activities of Tk neurons. Data are plotted in 30-min bins, with white and black bars on the x axis indicating 12-h light and 12-h dark conditions, respectively.

(D) Sleep profiles of Tk mutant and WT flies (n = 48 for each genotype).

(E) Sleep profiles after the activities of CCHa1-expressing neurons were increased by NaChBac or decreased by Kir2.1.

(F) Sleep profiles of *CCHa1* mutant and WT flies (n = 24 for WT, 20 for *CCHa1*).

which is a major small-molecule transmitter in insects though only a trace amine in mammals. OA is synthesized by *TβH* (Roeder, 2005; Monastirioti et al., 1996). We used CRISPR-Cas9 to replace the coding region of *Oa2* and *Octβ2R* with that of Gal4 to generate their null mutants. With these mutants, we confirmed that sleep phenotype in *Octβ2R* null mutants, but not in *Oa2* null mutants (Figures 6 A and 6B). Sleep durations of *TβH* and *Octβ2R* mutants were approximately half that of wild-type (WT) flies (Figures 6A and 6B) due to decreased nighttime sleep (Figure S7B), but not daytime sleep (Figure S7A). Nighttime sleep loss was attributable to shorter bout duration and reduced bout number (Figures S7D and S7F). Sleep was not affected in $Octβ3R^{-/-}$ or $Oct\text{-}TyrR^{-/-}$ mutants, but daytime sleep was increased in *OAMB* null mutants (Figures 6A, 6B,

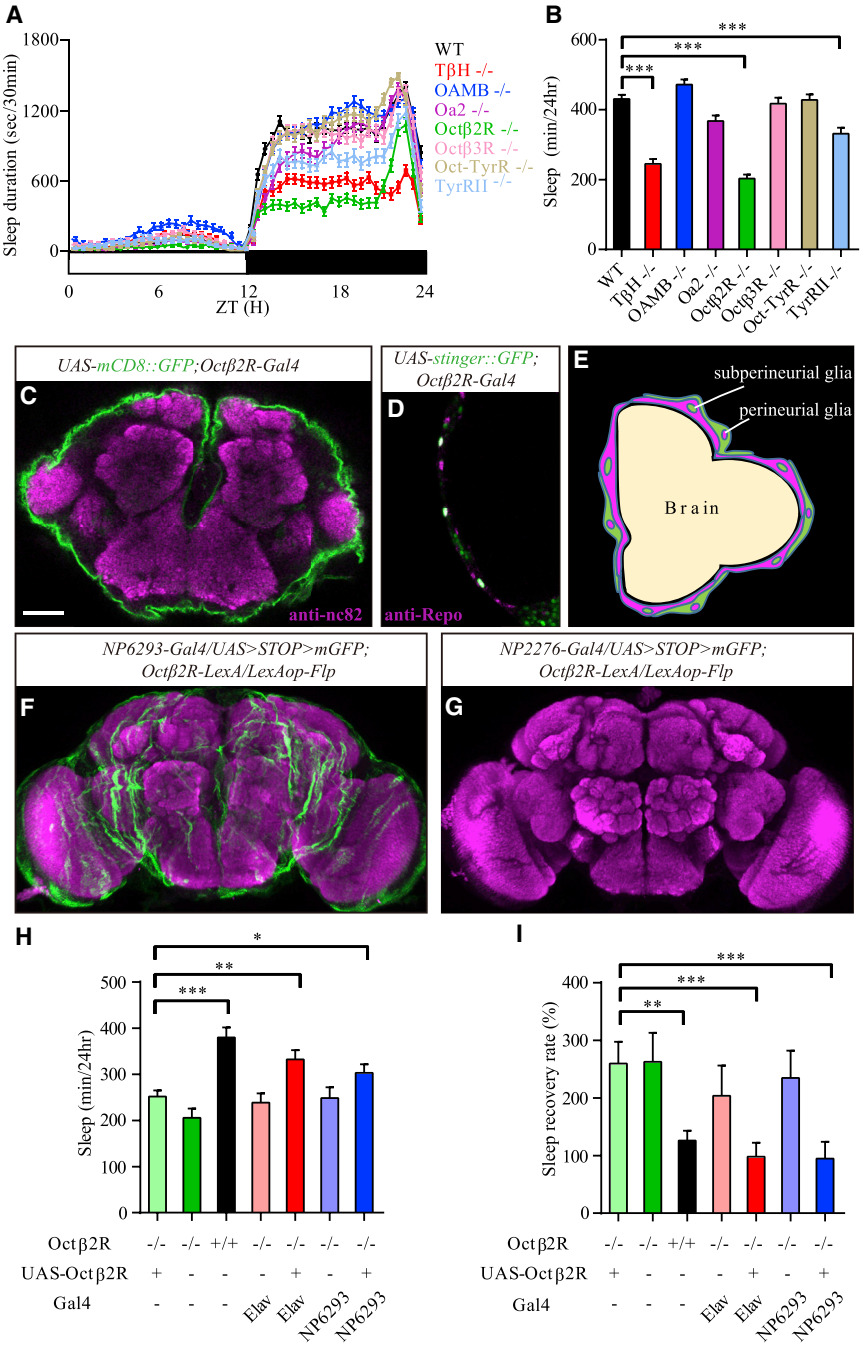

Figure 6. Genetic Rescue of Sleep Phenotypes in *Octβ2R* Mutants

(A) Sleep profiles of octopaminergic mutants.

(B) Statistical analyses of sleep phenotypes in octopaminergic mutants. Total sleep was decreased by half in *TβH* and *Octβ2R* mutants (n = 95 for WT, n = 94 for *TβH*, n = 95 for *OAMB*, n = 85 for *Oa2*, n = 94 for *Octβ2R*, n = 85 for *Octβ3R*, n = 89 for *Oct-TyrR* , and n = 91 for *TyrRII*). Mean ± SEM is shown. The Kruskal-Wallis test followed by Dunn's post test was used. *, **, and *** denote $p < 0.05$, $p < 0.01$, and $p < 0.001$, respectively.

(C) Localization of Octβ2R-positive glial cells revealed with *UAS-mCD8::GFP*.

(D) Co-staining of the nuclear GFP in *UAS-stinger::GFP* driven by *Octβ2R-Gal4* with immunostaining by the anti-Repo antibody.

(E) A cartoon showing the morphology and localization of surface-associated subperineurial and perineurial glia in *Drosophila*.

(F) Intersectional analysis of *Octβ2R-LexA* with *NP6293-Gal4* indicated that *Octβ2R* was expressed in perineurial glia. Green, GFP; magenta, nc82. Scale bars, 30 μm.

(G) Intersectional analysis of *Octβ2R-LexA* with *NP2276-Gal4*. No intersectional signal was detected in subperineurial glia. Green, GFP; magenta, nc82.

(H and I) Genetic rescue of sleep phenotypes in $Octβ2R^{-/-}$ mutant flies. *UAS-Octβ2R* cDNA was driven by the neuronal-specific *Elav-Gal4* or the perineurial-glial-specific *NP6293-Gal4* in $Octβ2R^{-/-}$ mutants. Sleep loss could be partially rescued with either Gal4 line (H), while sleep recovery after deprivation could be rescued to WT levels with either Gal4 line (I) (n = 106 for *UAS-Octβ2R; Octβ2R*$^{-/-}$, n = 66 for $Octβ2R^{-/-}$, n = 68 for WT, n = 96 for *Elav-Gal4::Octβ2R*$^{-/-}$, n = 110 for *Elav-Gal4;UAS-Octβ2R;Octβ2R*$^{-/-}$, n = 77 for *NP6293;Octβ2R*$^{-/-}$, and n = 110 for *NP6293-Gal4, UAS-Octβ2R; Octβ2R*$^{-/-}$). Mean ± SEM is shown. The Kruskal-Wallis test followed by Dunn's post test was used. ** and *** denote $p < 0.01$ and $p < 0.001$, respectively.

S7A, and S7B). Sleep recovery after deprivation was increased in *TβH* and *Octβ2R* mutant flies (Figures S7G and S7H). Taken together, our results suggest that OA promotes sleep through Octβ2R. It is unclear why $OAMB^{-/-}$ and *TβH* mutants had an opposite phenotype, though it remains to be investigated whether subsets of *TβH* neurons could have opposite roles, with Octβ2R mediating sleep promotion and OAMB mediating sleep inhibition.

We found Octβ2R in both glial cells and neurons (Figures 3E–3J). The morphology and localization of Octβ2R-expressing glial cells indicated that they were surface-associated glia (Figures 6C and 6D). There are two types of surface-associated glia in *Drosophila*, the subperneurial glia and perineurial glia, which could be labeled by *NP2276-Gal4* and *NP6293-Gal4*, respectively (Awasaki et al., 2008) (Figure 6E). Intersectional analysis of the *Octβ2R-LexA* revealed *Octβ2R* was in perineurial glia, but not subperineurial glia (Figures 6F and 6G).

We further carried out genetic rescue experiments by reintroducing Octβ2R into $Octβ2R^{-/-}$ mutants either with the perineurial glial *NP6293-Gal4* or the neuronal *Elav-Gal4* driving *UAS-Octβ2R*. The sleep-decrease phenotype was partially rescued by either *NP6293-Gal4* or *Elav-Gal4* (Figure 6H). The sleep-rebound phenotype of *Octβ2R* mutants was also partially rescued by reintroduction of Octβ2R into neurons or glial cells (Figure 6I). Thus, both neurons and perineurial glia cells are required for Octβ2R-mediated OA regulation of sleep in flies.

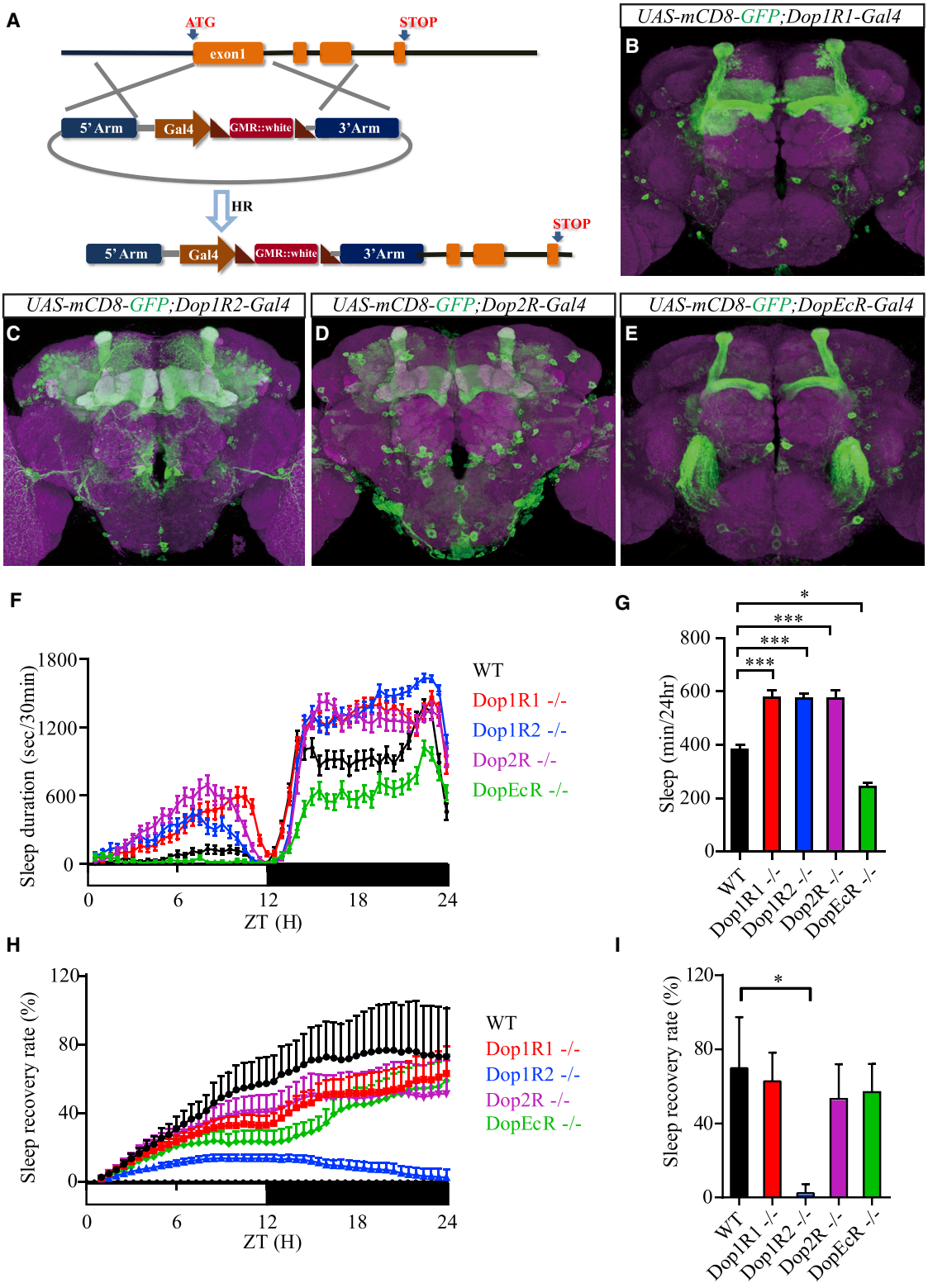

Figure 7. Expression of DRs and Their Functional Roles in Sleep

(A) Ends-out gene targeting was used to replace the endogenous gene from the first exon with Gal4, attP, and *loxP* flanking the selection marker GMR::miniwhite (Rong and Golic, 2000, 2001).

(legend continued on next page)

Regulation of Sleep by DRs

Our pilot screen of 147 KOs implicated all four DRs in sleep regulation, with *Dop1R1*, *Dop1R2*, and *Dop2R* inhibiting sleep and *DopEcR* promoting sleep (Table S3). We generated null mutants for the DRs by replacing the first coding exon of *Dop1R1*, *Dop1R2*, and *DopEcR* and the last seven common exons of *Dop2R* with Gal4 (Figure 7A) (Rong and Golic, 2000, 2001). We also generated a null mutant for TH (aka *pale*) and found the *pale* null mutants were lethal, consistent with a previous report (Friggi-Grelin et al., 2003).

We analyzed the expression patterns for these KO Gal4 lines by crossing them to *UAS-mCD8-GFP* for membrane labeling (Figures 7B–7E), *UAS-Stinger* for nuclear labeling (Figures S10A–S10E), *UAS-nSyb-eGFP* for axonal labeling (Figures S9F–S9J), and *UAS-Dscam17.1-GFP* for dendritic labeling (Figures S10K–S10O). The pattern shown by *ple-Gal4* was consistent with previous reports (Budnik and White, 1988; Mao and Davis, 2009) (Figure S10). Each DR had a distinct pattern (Figures 7B–7E and S10). In the MB, *Dop1R1* in the γ and αβ lobes (Figures S10G1–S10G3); *Dop1R2* strongly in the γ and αβ lobes but weakly in the α′β′ lobes (Figures S10H1–S10H3); *Dop2R* in all lobes (Figures S10I1–S10I3); *DopEcR* strongly in the αβ lobes but weakly in the γ lobe (Figures S10J1–S10J3). All four DRs projected to the fan-shaped bodies (FSBs) (Figures S10G4, S10H4, S10I4, and S10J4). Axon labeling showed *Dop1R2* and *DopEcR* projection to the antennal mechanosensory and motor center (AMMC) (Figures S10H, S10J, S10Q5, and S10S5). Dendrite labeling showed *Dop1R1* and *DopEcR* innervation of specific glomeruli in the AL (Figures S10L and S10O).

The sleep phenotypes observed in the CCT KO lines were confirmed in the null mutants and were increased in $Dop1R1^{-/-}$, $Dop1R2^{-/-}$, and $Dop2R^{-/-}$ null mutants but decreased in $DopEcR^{-/-}$ null mutants (Figures 7F and 7G). Both daytime and nighttime sleep durations were increased in $Dop1R1^{-/-}$, $Dop1R2^{-/-}$, and $Dop2R^{-/-}$ mutants (Figures 7F, 7G, S9A, and S9B). Daytime sleep bout numbers were increased in $Dop1R1^{-/-}$, $Dop1R2^{-/-}$, and $Dop2R^{-/-}$ mutants (Figure S9C). Nighttime sleep bout number was increased only in $Dop1R2^{-/-}$ mutants (Figure S9D). Daytime sleep bout durations were increased in $Dop1R1^{-/-}$, $Dop1R2^{-/-}$ and $Dop2R^{-/-}$ mutants (Figure S9E). Nighttime sleep bout durations were increased in $Dop1R1^{-/-}$ and $Dop2R^{-/-}$ mutants (Figure S9F). $DopEcR^{-/-}$ mutants often displayed phenotypes opposite those of $Dop1R1^{-/-}$, $Dop1R2^{-/-}$, and $Dop2R^{-/-}$ mutants. Nighttime sleep, but not daytime sleep, was significantly decreased in $DopEcR^{-/-}$ mutants (Figures 7F, 7G, S9A, and S9B). Nighttime sleep bout duration (Figure S9F), but not bout number (Figure S9C), was reduced in $DopEcR^{-/-}$ mutants.

As shown previously (Liu et al., 2012; Pfeiffenberger and Allada, 2012), L-3,4-dihydroxyphenylalanine (L-DOPA) feeding led to a sleep loss ratio of nearly 100% (Figures S9G and S9H). The effect of L-DOPA on sleep was dependent on DRs, with the sleep loss ratio reduced to 44%, 38%, and 62% in $Dop1R1^{-/-}$, $Dop1R2^{-/-}$, and $Dop2R^{-/-}$ mutants, respectively (Figures S9G and S9H). *DopEcR* was not required for L-DOPA inhibition of sleep (Figures S9G and S9H).

Only one DR was found to be involved in sleep recovery after deprivation. After 12-h nighttime sleep deprivation by mechanical stimuli, WT flies recovered nearly 80% of sleep the following day (Figures 7H and 7I). Sleep recovery was not significantly different between $Dop1R1^{-/-}$, $Dop2R^{-/-}$, or $DopEcR^{-/-}$ mutants and WT flies (Figures 7H and 7I). However, sleep recovery was significantly reduced in $Dop1R2^{-/-}$ mutants (Figures 7H and 7I).

To examine cells in which *Dop2R* functions in sleep regulation, we utilized the Gal4/UAS system to rescue the sleep increase phenotype of $Dop2R^{-/-}$ mutants. We expressed *Dop2R* cDNA to subsets of neurons known to be involved in sleep regulation, including dorsal FSB (dFSB) neurons (with *23E10-Gal4*), dopaminergic neurons (with *TH-Gal4*), ventral lateral neurons (with *pdf-Gal4*), MB neurons (with *c739-Gal4*, *c309-Gal4*, *NP1131-Gal4*, or *c305a-Gal4*), and pars intercerebralis (PI) neurons (with *dilp2-Gal4*) (Figure 8A). Only *dilp2-Gal4* rescued the phenotype of *Dop2R* mutants (Figure 8A).

dilp2-Gal4 is expressed in 7 PI neurons per hemisphere of the brain. PI neurons expressing DH44, SIFamide, and Rhomboid (*c767* and *50Y*) are known to regulate sleep and circadian rhythm (Cavanaugh et al., 2014; Foltenyi et al., 2007; Park et al., 2014). We used the corresponding Gal4 drivers to test for involvement of *Dop2R* in these neurons (Figure 8B). In addition to Dilp2 neurons, restoration of *Dop2R* expression in SIFa neurons by *SIFa-Gal4* also partially rescued the *Dop2R* mutant phenotype, indicating that Dilp2 and SIFa neurons mediate *Dop2R* inhibition of sleep (Figure 8B).

To examine whether *Dop2R* is expressed in Dilp2 and SIFa neurons, we used *Dop2R-Gal4* to drive *UAS-Stinger* for nuclear expression of GFP and antibodies for Dilp2 (Figures 8C–8E) or SIFa immunostaining (Figures 8F–8H). We found *Dop2R* expression in Dilp2 (Figure 8E) and SIFa neurons (Figure 8H). These results support that *Dop2R* functions in Dilp2 and SIFa neurons to regulate sleep. Thus, it is possible to trace from a receptor to other neuropeptides, facilitating dissection of neurochemical circuitry.

(B–E) Expression patterns of *UAS-mCD8-GFP* driven by *Dop1R1-Gal4* (B), *Dop1R2-Gal4* (C), *Dop2R-Gal4* (D), and *DopEcR-Gal4* (E). Green, GFP; Magenta, nc82.

(F) Sleep profiles of DR mutant flies. Daytime and nighttime sleep durations were increased in $Dop1R1^{-/-}$, $Dop1R2^{-/-}$, and $Dop2R^{-/-}$ mutants but decreased in $DopEcR^{-/-}$ mutants (n = 47 for WT, n = 47 for $Dop1R1^{-/-}$, n = 47 for $Dop1R2^{-/-}$, n = 46 for $Dop2R^{-/-}$, and n = 44 for $DopEcR^{-/-}$ mutants).

(G) Statistical analysis of total sleep duration in 24 h. Sleep durations were significantly increased in $Dop1R1^{-/-}$, $Dop1R2^{-/-}$, and $Dop2R^{-/-}$ mutants but significantly decreased in $DopEcR^{-/-}$ mutants.

(H) After overnight sleep deprivation for 12 h by mechanical stimuli, sleep recovery accumulation curves were plotted on the following day for the WT (n = 31), $Dop1R1^{-/-}$ (n = 32), $Dop1R2^{-/-}$ (n = 30), $Dop2R^{-/-}$ (n = 43), and $DopEcR^{-/-}$ (n = 35) mutant flies.

(I) Statistical analysis of sleep recovery rate in WT and DR mutants. Only $Dop1R2^{-/-}$ mutants showed significantly reduced sleep recovery after deprivation. *, **, and *** denote $p < 0.05$, $p < 0.01$, and $p < 0.001$, respectively.

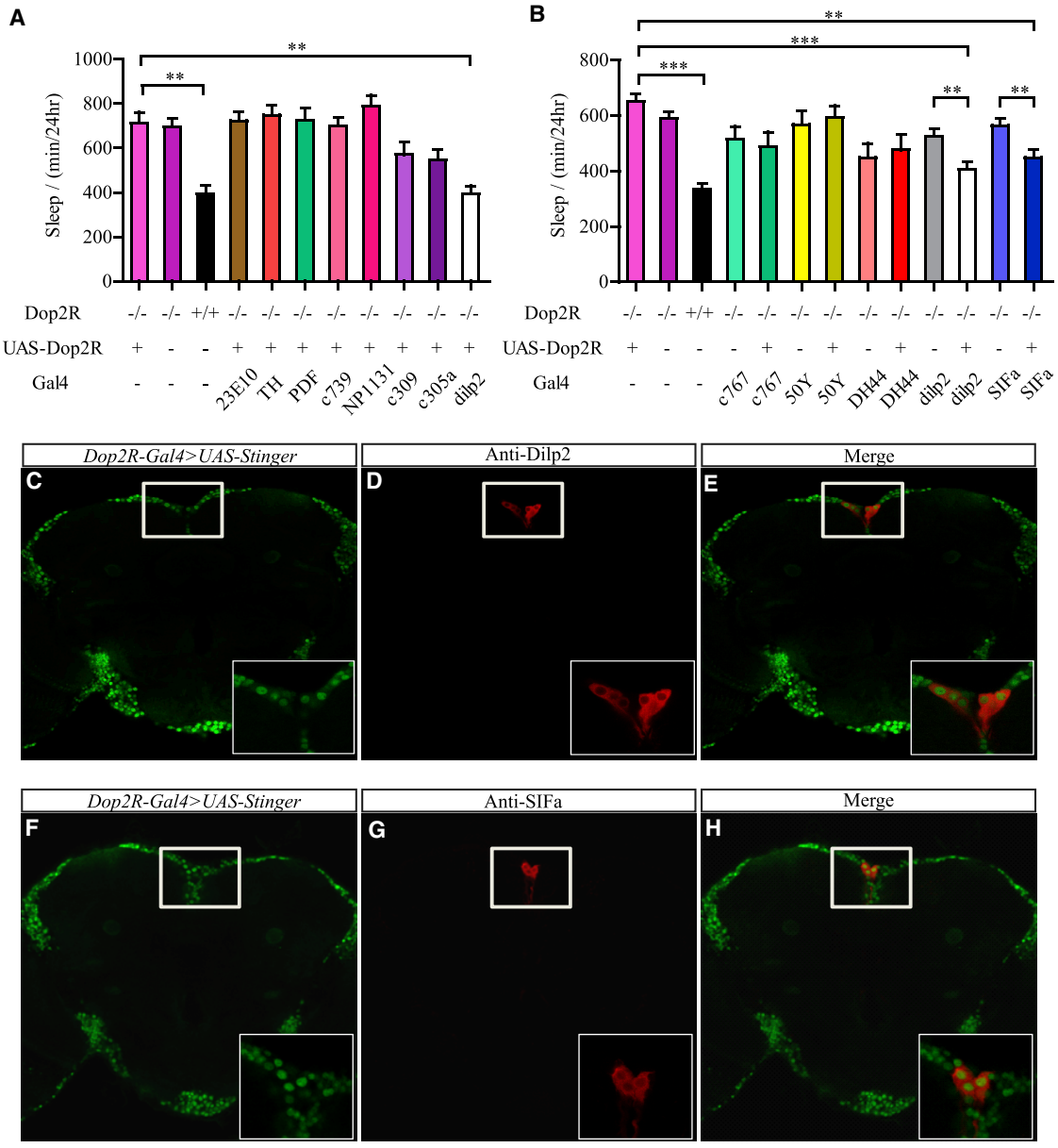

Figure 8. Expression and Function of Dop2R in Dilp2 or SIFa Neurons

(A) The sleep-increase phenotype in *Dop2R*$^{-/-}$ mutants could be rescued when expression of *UAS-Dop2R* was driven by *Dilp2-Gal4*, but not by *23E10-Gal4* (dFSB neurons), *TH-Gal4* (DA neurons), *pdf-Gal4* (LNvs), *c739*, *c309*, *NP1131*, or *c305a* (MB neurons). n = 23–24 for all lines except for *c309-Gal4* (n = 15).

(B) The sleep phenotype in *Dop2R*$^{-/-}$ mutants could be rescued when expression of UAS-Dop2R was driven by *Dilp2-Gal4* (n = 48) or *SIFa-Gal4* (n = 38), but not with other Gal4 drivers for subsets of PI neurons, including *c767*, *50Y*, and *DH44* (n = 24).

(C–E) Colocalization of Dop2R with Dilp2: *UAS-Stinger GFP* driven by *Dop2R-Gal4* (C) was found to overlap with immunostaining by the anti-Dilp2 antibody (D), and all the Dilp2 positive neurons expressed Dop2R (E). Green, GFP; Red, Dilp2.

(F–H) Colocalization of *Dop2R* with SIFa: *UAS-Stinger GFP* driven by *Dop2R-Gal4* (F) overlapped with anti-SIFa immunostaining (G) and all the SIFa positive neurons expressed Dop2R (H). Green, GFP; red, SIFa.

DISCUSSION

The CCT, Chemoconnectomics, and CCT Lines

The CCT is a new concept that reflects a biologically important entity hitherto underappreciated as a whole though intensively studied individually. Chemoconnectomics is a novel approach to study the functional significance of the CCT as a biologically meaningful entry point to dissect neural circuits underlying behavior and cognition. Chemoconnectomics lines such as those presented here for *Drosophila* should be generated in other animals for general applications in molecular studies of behavior and cognition and genetic dissection of the neural circuitry underlying behavior and cognition.

The CCT can be compared in several aspects. For connectomics, the CCT can be compared to existing ones, including EM, MRI, and virally mediated approaches. The advantages of the CCT over EM and MRI are that the CCT has molecular resolution and can be used for molecular and cellular manipulations, as well as genetic intersections. Compared to viral injections, the CCT is more reproducible in different animals, more comprehensive in covering all cells expressing the same gene, and more definitive in terms of knowing that every cell type with known neurochemistry has been covered. The CCT will complement all of these approaches. For example, many viral injections use CCT lines. When protein-tagged EM markers are widely accepted, the CCT can be used for EM directly. In non-human primates, the CCT can also be combined with MRI.

For genetic labeling of neurons and neuronal circuitry, the CCT can be compared with minos-mediated integration cassette (MiMIC) (Venken et al., 2011) and genomic insertions of Gal4 (Jenett et al., 2012). The CCT includes both KO and KI, with the latter highly selective in targeting only genes related to transmitters, modulators, neuropeptides, and their receptors and placing Gal4 (and others) in frame at the C terminus of an endogenous protein. MiMIC placed Gal4 through splicing acceptor sites, which may or may not be accurate in reporting the patterns of endogenous genes, and such placements also do not guarantee functional inactivation. Placement of Gal4 every 2 kb in the genome provides more patterns, but with uncertain biological meaning, because such insertions often do not reflect patterns of endogenous proteins.

For genetic studies of behavior and cognition, the CCT can be compared to saturation mutagenesis. Saturation mutagenesis is powerful in yeast, worms, and flies, but screening of all genes is more time consuming and more expensive than CCT. These limit the applications of saturation mutagenesis, which has not become a routine in mammals. Once generated, CCT lines are simple and inexpensive to use. Saturation mutagenesis is an one-time application, but each mutagenesis has to be set up anew. CCT tools can be used repeatedly (and, if necessary, comparatively). The CCT can certainly be established in mammals and is imaginable in non-human primates. Saturation mutagenesis covers many genes that do not provide mechanistic insights, even if proven to be involved, whereas the CCT is focused on molecules and cells involved in neural signaling, providing insights into neural signaling and pathways. This will be particularly helpful in mammals.

Coexistence of Transmitters, Modulators, and Neuropeptides in *Drosophila*

In all cases we have examined so far, each transmitter/modulator/neuropeptide coexists with another, though in different regions and with different combinations. This indicates that conditional KO and double and triple KO combinations will be helpful, although circuitry dissection can be done now with single mutations and intersections of two genes.

The simple version of Dale's principle (Dale, 1935; Eccles et al., 1954; Eccles, 1976) is known to be incorrect, because multiple transmitters, modulators, and neuropeptides coexist in the same neurons and sometimes in the same synaptic vesicles. The most common observation of co-transmission is the presence of a small-molecule transmitter and a neuropeptide in the same neuron (Hökfelt, 1991; Lundberg, 1996; Nusbaum et al., 2017), but the coexistence of two small-molecule transmitters has also been observed (Jonas et al., 1998). In mammals, examples of co-transmission include glycine with GABA (Jonas et al., 1998) and DA with GABA (Hirasawa et al., 2012). Glu has been found to be a co-transmitter with ACh (Herzog et al., 2004a, 2004b; Münster-Wandowski et al., 2016; Granger et al., 2017), DA (Dal Bo et al., 2004; Mendez et al., 2008; Tecuapetla et al., 2010; Zhang et al., 2015), and 5-HT (Schäfer et al., 2002).

Our CCT lines enable systematic investigations of coexistence in *Drosophila*. The intersection of TH with 24 KI Gal4 lines revealed that 16 transmitters and neuropeptides might coexist with DA (Figure 4).

In other organisms, it is presently difficult to conclude that one transmitter does not coexist with another. With the systematic nature of the CCT, we can now show that GABAergic inhibitory neurons do not contain either of the major excitatory transmitters (Glu or ACh) in the CNS of *Drosophila* (Figures 4L–4Q).

The presence of more than one transmitter/modulator/neuropeptide in the same neuron provides one of the reasons why manipulating neuronal activities is not equivalent to manipulating one transmitter. This was witnessed by our results that neuronal activation of by NaChBac or inhibition of neuronal activity by Kir2.1 could result in a phenotype that was either the same as or different from the phenotype of mutating a gene encoding a neuropeptide (Figures 5B–5F) or a small-molecule transmitter (data not shown) in sleep regulation. This provides a cautious note that underscores lessons previously learned from both mammalian (e.g., Wu and Palmiter, 2011) and *Drosophila* (e.g., Selcho et al., 2017) studies: for a specific neuronal cell type, manipulating its activity should be considered separately from results of manipulating single molecules.

Regulation of Sleep by DA

Sleep has been observed in every animal species studied to date (Campbell and Tobler, 1984. In mammals, sleep can be separated into different phases by electroencephalogram (EEG) and electromyogram (EMG) recordings (Aserinsky and Kleitman, 1953; Davis et al., 1937). In flies, sleep is usually monitored by locomotion (Hendricks et al., 2000; Shaw et al., 2000). DA regulates sleep in both mammals (Wisor et al., 2001; Lu et al., 2006; Eban-Rothschild et al., 2016; Qu et al., 2010) and flies (Kume et al., 2005; Qu et al., 2010; Liu et al., 2012; Ueno et al., 2012; Kayser et al., 2014; Seidner et al., 2015; Sitaraman et al., 2015; Nall et al., 2016; Pimentel et al., 2016).

We have constructed null mutants and KI GAL4 lines for TH and all four DRs. Homozygous $TH^{-/-}$ mutants were lethal, but DR mutants were viable and were studied behaviorally. Dop1R1, Dop1R2, and Dop2R suppresses sleep and mediates sleep loss induced by L-DOPA, whereas DopEcR promotes sleep (Figures 7F, 7G, S9G, and S9H). Dop1R2 is involved in sleep recovery after sleep deprivation (Figures 7H and 7I). Genetic rescue experiments indicated that Dop2R functions in Dilp2 and SIFa neurons to regulate sleep (Figures 8A and 8B). Previous results showed that sleep was reduced in *dilp2* mutants and in *SIFa* knockdown flies (Cong et al., 2015; Park et al., 2014). Because Dop2R is coupled to Gi (Hearn et al., 2002), the simplest

explanation is that DA inhibits neurons expressing Dop2R and thus inhibits neurons expressing either Dilp2 or SIFa.

The role of DopEcR in sleep is opposite to that expected from DA and also unrelated to L-DOPA feeding (Figure S9G), indicating that it may not be downstream of DA in sleep regulation. DopEcR can be activated by both DA and ecdysone. Previous reports showed that ecdysone feeding increased sleep (Ishimoto and Kitamoto, 2010).

Dop1R2 is necessary for sleep homeostasis (Figures 7H and 7I). Previous results suggest that *Dop1R2* knockdown in dFSB increased sleep (Pimentel et al., 2016) and that *cvc* at dFSB regulates homeostasis (Donlea et al., 2014). It will be interesting to investigate whether *Dop1R2* in dFSB regulates sleep homeostasis, possibly upstream of *cvc*.

Role of Glia in Regulating Sleep

Previous studies suggest a wake-promoting role for OA (Crocker and Sehgal, 2008; Crocker et al., 2010), which is different from our results. This difference may have resulted from the different methods used to measure sleep. Previous work used the *Drosophila* Activity Monitor (DAM)-based method, whereas we used the video-based method. We reanalyzed our video-based data using the DAM-based method and found that similar to the previous work, the sleep duration of $T\beta H^{-/-}$ mutants was significantly increased (Figure S8). The sleep duration of $Oct\beta 2R^{-/-}$ mutants was also significantly increased when analyzed by the DAM method (Figure S8). Because the DAM-based method only measures fly movement across the midpoint of a tube (excluding activities in either end of the tube), it is less sensitive in motion detection than the video-based method. We thus conclude that sleep is reduced in both $T\beta H^{-/-}$ and $Oct\beta 2R^{-/-}$ mutants.

Our *Octβ2R* KI line indicates that *Octβ2R* is expressed in both neuronal and glial cells (Figures 6C–6G). Cells expressing *Octβ2R* intersected with the glial Gal4 line NP6293, but not the other glial Gal4 line NP2276. Functionally, sleep loss in $Oct\beta 2R^{-/-}$ mutants could be rescued partially by either Elav-Gal4- or NP6293-driven expression of UAS-*Octβ2R*. The sleep recovery after deprivation phenotype in $Oct\beta 2R^{-/-}$ mutants could also be partially rescued by the expression of UAS-*Octβ2R* in either neuronal or glial cells. These results support a role for both neurons and glial cells in mediating sleep regulation.

In *Drosophila*, glia have been implicated in regulating the circadian rhythm (Suh and Jackson, 2007; Ng et al., 2011, 2016). Gap junction rhythms driven by a circadian clock in the perineurial glia were reported recently (Zhang et al., 2018). Reduction of GABA transaminase, an enzyme responsible for degrading GABA, in glia decreased sleep (Chen et al., 2015), indicating that GABA in glial cells inhibits sleep. Reduction of the transmembrane receptor Notch in glia impaired sleep homeostasis (Seugnet et al., 2011). It will be interesting to further investigate mechanisms underlying sleep regulation by glia. OA has been previously known to function through the astrocytic Oct-TyrR receptor to regulate the startle responses in flies (Ma et al., 2016). Taken together with our new results, glia therefore appear to mediate multiple functions of OA.

In our CCT screen, we have so far detected glial expression of only one neuropeptide (Figure 3). It will be interesting to study its function and its target cells.

STAR★METHODS

Detailed methods are provided in the online version of this paper and include the following:

- KEY RESOURCES TABLE
- CONTACT FOR REAGENT AND RESOURCE SHARING
- EXPERIMENTAL MODEL AND SUBJECT DETAILS
  - Fly Lines and Rearing Conditions
- METHOD DETAILS
  - Gene Selection
  - Molecular Biology
  - Generation of KO, KI and Transgenic Lines
  - Behavioral Assays
  - L-DOPA Feeding
  - Immunohistochemistry and Confocal Imaging
- QUANTIFICATION AND STATISTICAL ANALYSIS

SUPPLEMENTAL INFORMATION

Supplemental Information includes ten figures and three tables and can be found with this article online at https://doi.org/10.1016/j.neuron.2019.01.045.

ACKNOWLEDGMENTS

We are grateful to Drs. J. Ni and Dr. G. Gao for providing us CRISPR-Cas9 plasmids and flies; Drs. R. Allada, B. Dickson, J. Dubnau, P. Garrity, L. Griffith, C.H. Lee, J. Hirsh, J. Veenstra, and C.F. Wu for sharing flies; and Drs. Z.-F. Gong and J. Veenstra for sharing antibodies. This work was supported by the Beijing Commission of Science and Technology (Z151100003915121 to W. Z.), the Beijing Advanced Innovation Center for Genomics, and the National Natural Science Foundation of China (Project 31421003 to Y.R.) for grant support.

AUTHOR CONTRIBUTIONS

B.D. and Y.C. performed the majority of experiments and data analysis. Q.L. carried out experiments with TH and DRs. X.L. carried out experiments with octopamine receptors. B.L. carried out experiments with Ado. Y.Q. performed the sleep screen experiment. R.X. and J.H. were involved in the DR experiments and some early parts of this project. R.M. performed immunostaining for protein-trap flies. E.Z. designed the targeting vector for D-serine-related flies and developed sleep analysis programs. B.D., Q.L., X.L., and Y.R. wrote the manuscript.

DECLARATION OF INTERESTS

The authors declare no competing interests.

Received: June 7, 2018
Revised: November 2, 2018
Accepted: January 17, 2019
Published: February 21, 2019

REFERENCES

Abruzzi, K.C., Zadina, A., Luo, W., Wiyanto, E., Rahman, R., Guo, F., Shafer, O., and Rosbash, M. (2017). RNA-seq analysis of Drosophila clock and non-clock neurons reveals neuron-specific cycling and novel candidate neuropeptides. PLoS Genet. *13*, e1006613.

Aserinsky, E., and Kleitman, N. (1953). Regularly occurring periods of eye motility, and concomitant phenomena, during sleep. Science *118*, 273–274.

Awasaki, T., Lai, S.L., Ito, K., and Lee, T. (2008). Organization and postembryonic development of glial cells in the adult central brain of Drosophila. J. Neurosci. *28*, 13742–13753.

Baines, R.A., Uhler, J.P., Thompson, A., Sweeney, S.T., and Bate, M. (2001). Altered electrical properties in Drosophila neurons developing without synaptic transmission. J. Neurosci. *21*, 1523–1531.

Barger, G., and Dale, H.H. (1910). A third active principle in ergot extracts. Proc. Chem. Soc. Lond *26*, 128–129.

Bargmann, C.I., and Marder, E. (2013). From the connectome to brain function. Nat. Methods *10*, 483–490.

Beier, K.T., Steinberg, E.E., Deloach, K.E., Xie, S., Miyamichi, K., Schwarz, L., Gao, X.J., Kremer, E.J., Malenka, R.C., and Luo, L. (2015). Circuit architecture of VTA dopamine neurons revealed by systematic input-output mapping. Cell *162*, 622–634.

Boulland, J.L., Jenstad, M., Boekel, A.J., Wouterlood, F.G., Edwards, R.H., Storm-Mathisen, J., and Chaudhry, F.A. (2009). Vesicular glutamate and GABA transporters sort to distinct sets of vesicles in a population of presynaptic terminals. Cereb. Cortex *19*, 241–248.

Broeck, J.V. (2001). Neuropeptides and their precursors in the fruitfly, Drosophila melanogaster. Peptides *22*, 241–254.

Budnik, V., and White, K. (1988). Catecholamine-containing neurons in Drosophila melanogaster: distribution and development. J. Comp. Neurol. *268*, 400–413.

Burg, M.G., Sarthy, P.V., Koliantz, G., and Pak, W.L. (1993). Genetic and molecular identification of a Drosophila histidine decarboxylase gene required in photoreceptor transmitter synthesis. EMBO J. *12*, 911–919.

Campbell, S.S., and Tobler, I. (1984). Animal sleep: a review of sleep duration across phylogeny. Neurosci. Biobehav. Rev. *8*, 269–300.

Carlsson, A., Lindqvist, M., Magnusson, T., and Waldeck, B. (1958). On the presence of 3-hydroxytyramine in brain. Science *127*, 471.

Cavanaugh, D.J., Geratowski, J.D., Wooltorton, J.R., Spaethling, J.M., Hector, C.E., Zheng, X., Johnson, E.C., Eberwine, J.H., and Sehgal, A. (2014). Identification of a circadian output circuit for rest:activity rhythms in Drosophila. Cell *157*, 689–701.

Chen, W.F., Maguire, S., Sowcik, M., Luo, W., Koh, K., and Sehgal, A. (2015). A neuron-glia interaction involving GABA transaminase contributes to sleep loss in sleepless mutants. Mol. Psychiatry *20*, 240–251.

Cole, S.H., Carney, G.E., McClung, C.A., Willard, S.S., Taylor, B.J., and Hirsh, J. (2005). Two functional but noncomplementing Drosophila tyrosine decarboxylase genes: distinct roles for neural tyramine and octopamine in female fertility. J. Biol. Chem. *280*, 14948–14955.

Cong, X., Wang, H., Liu, Z., He, C., An, C., and Zhao, Z. (2015). Regulation of sleep by insulin-like peptide system in Drosophila melanogaster. Sleep (Basel) *38*, 1075–1083.

Cooper, J.R., Bloom, F.E., and Roth, R.H. (2003). The Biochemical Basis of Neuropharmacology, Eighth Edition (Oxford University Press).

Corey, J.L., Quick, M.W., Davidson, N., Lester, H.A., and Guastella, J. (1994). A cocaine-sensitive Drosophila serotonin transporter: cloning, expression, and electrophysiological characterization. Proc. Natl. Acad. Sci. USA *91*, 1188–1192.

Crocker, A., and Sehgal, A. (2008). Octopamine regulates sleep in Drosophila through protein kinase A-dependent mechanisms. J. Neurosci. *28*, 9377–9385.

Crocker, A., Shahidullah, M., Levitan, I.B., and Sehgal, A. (2010). Identification of a neural circuit that underlies the effects of octopamine on sleep:wake behavior. Neuron *65*, 670–681.

Croset, V., Treiber, C.D., and Waddell, S. (2018). Cellular diversity in the *Drosophila* midbrain revealed by single-cell transcriptomics. eLife *7*, 1–31.

Curtis, D.R., Phillis, J.W., and Watkins, J.C. (1959). Chemical excitation of spinal neurones. Nature *183*, 611–612.

Dal Bo, G., St-Gelais, F., Danik, M., Williams, S., Cotton, M., and Trudeau, L.-E. (2004). Dopamine neurons in culture express VGLUT2 explaining their capacity to release glutamate at synapses in addition to dopamine. J. Neurochem. *88*, 1398–1405.

Dale, H.H. (1914). The action of certain esters and ethers of choline, and their relation to muscarine. J. Pharmacol. Exp. Ther. *6*, 147–190.

Dale, H. (1935). Pharmacology and nerve-endings. Proc. R. Soc. Med. *28*, 319–332.

Dale, H.H., and Feldberg, W. (1934). The chemical transmission of secretory impulses to the sweat glands of the cat. J. Physiol. *82*, 121–128.

Daniels, R.W., Collins, C.A., Gelfand, M.V., Dant, J., Brooks, E.S., Krantz, D.E., and DiAntonio, A. (2004). Increased expression of the Drosophila vesicular glutamate transporter leads to excess glutamate release and a compensatory decrease in quantal content. J. Neurosci. *24*, 10466–10474.

Davis, H., Davis, P.A., Loomis, A.L., Harvey, E.N., and Hobart, G. (1937). Changes in human brain potentials during the Onset of Sleep. Science *86*, 448–450.

Demchyshyn, L.L., Pristupa, Z.B., Sugamori, K.S., Barker, E.L., Blakely, R.D., Wolfgang, W.J., Forte, M.A., and Niznik, H.B. (1994). Cloning, expression, and localization of a chloride-facilitated, cocaine-sensitive serotonin transporter from Drosophila melanogaster. Proc. Natl. Acad. Sci. USA *91*, 5158–5162.

Dolezelova, E., Nothacker, H.P., Civelli, O., Bryant, P.J., and Zurovec, M. (2007). A Drosophila adenosine receptor activates cAMP and calcium signaling. Insect Biochem. Mol. Biol. *37*, 318–329.

Donlea, J.M., Pimentel, D., and Miesenböck, G. (2014). Neuronal machinery of sleep homeostasis in Drosophila. Neuron *81*, 860–872.

Eban-Rothschild, A., Rothschild, G., Giardino, W.J., Jones, J.R., and de Lecea, L. (2016). VTA dopaminergic neurons regulate ethologically relevant sleep-wake behaviors. Nat. Neurosci. *19*, 1356–1366.

Eccles, J. (1976). From electrical to chemical transmission in the central nervous system. Notes Rec. R. Soc. Lond. *30*, 219–230.

Eccles, J.C., Fatt, P., and Koketsu, K. (1954). Cholinergic and inhibitory synapses in a pathway from motor-axon collaterals to motoneurones. J. Physiol. *126*, 524–562.

El Mestikawy, S., Wallén-Mackenzie, A., Fortin, G.M., Descarries, L., and Trudeau, L.E. (2011). From glutamate co-release to vesicular synergy: vesicular glutamate transporters. Nat. Rev. Neurosci. *12*, 204–216.

Elliot, T.R. (1904). On the action of adrenalin. Proc. Phys. Soc. *31*, 20–21.

Erspamer, V., and Vialli, M. (1937). Ricerche sul secreto delle cellule enterocromaffini. Boll Soc Med-chir Pavia *51*, 357–363.

Fattorini, G., Verderio, C., Melone, M., Giovedì, S., Benfenati, F., Matteoli, M., and Conti, F. (2009). VGLUT1 and VGAT are sorted to the same population of synaptic vesicles in subsets of cortical axon terminals. J. Neurochem. *110*, 1538–1546.

Fei, H., Chow, D.M., Chen, A., Romero-Calderón, R., Ong, W.S., Ackerson, L.C., Maidment, N.T., Simpson, J.H., Frye, M.A., and Krantz, D.E. (2010). Mutation of the Drosophila vesicular GABA transporter disrupts visual figure detection. J. Exp. Biol. *213*, 1717–1730.

Ffrench-Constant, R.H., Mortlock, D.P., Shaffer, C.D., MacIntyre, R.J., and Roush, R.T. (1991). Molecular cloning and transformation of cyclodiene resistance in Drosophila: an invertebrate gamma-aminobutyric acid subtype A receptor locus. Proc. Natl. Acad. Sci. USA *88*, 7209–7213.

Foltenyi, K., Greenspan, R.J., and Newport, J.W. (2007). Activation of EGFR and ERK by rhomboid signaling regulates the consolidation and maintenance of sleep in Drosophila. Nat. Neurosci. *10*, 1160–1167.

Frenkel, L., Muraro, N.I., Beltrán González, A.N., Marcora, M.S., Bernabó, G., Hermann-Luibl, C., Romero, J.I., Helfrich-Förster, C., Castaño, E.M., Marino-Busjle, C., et al. (2017). Organization of circadian behavior relies on glycinergic transmission. Cell Rep. *19*, 72–85.

Friggi-Grelin, F., Iché, M., and Birman, S. (2003). Tissue-specific developmental requirements of Drosophila tyrosine hydroxylase isoforms. Genesis *35*, 175–184.

Gibson, D.G., Young, L., Chuang, R.Y., Venter, J.C., Hutchison, C.A., 3rd, and Smith, H.O. (2009). Enzymatic assembly of DNA molecules up to several hundred kilobases. Nat. Methods *6*, 343–345.

Glasser, M.F., Smith, S.M., Marcus, D.S., Andersson, J.L.R., Auerbach, E.J., Behrens, T.E.J., Coalson, T.S., Harms, M.P., Jenkinson, M., Moeller, S., et al. (2016). The Human Connectome Project's neuroimaging approach. Nat. Neurosci. *19*, 1175–1187.

Granger, A.J., Wallace, M.L., and Sabatini, B.L. (2017). Multi-transmitter neurons in the mammalian central nervous system. Curr. Opin. Neurobiol. *45*, 85–91.

Greenspan, R.J. (1980). Mutations of cholineacetyltransferase and associated neural defects in Drosophila melanogaster. J. Comp. Physiol. *137*, 83–92.

Groth, A.C., Fish, M., Nusse, R., and Calos, M.P. (2004). Construction of transgenic Drosophila by using the site-specific integrase from phage phiC31. Genetics *166*, 1775–1782.

Han, C., Jan, L.Y., and Jan, Y.N. (2011). Enhancer-driven membrane markers for analysis of nonautonomous mechanisms reveal neuron-glia interactions in Drosophila. Proc. Natl. Acad. Sci. USA *108*, 9673–9678.

Hauser, A.S., Attwood, M.M., Rask-Andersen, M., Schiöth, H.B., and Gloriam, D.E. (2017). Trends in GPCR drug discovery: new agents, targets and indications. Nat. Rev. Drug Discov. *16*, 829–842.

Hearn, M.G., Ren, Y., McBride, E.W., Reveillaud, I., Beinborn, M., and Kopin, A.S. (2002). A Drosophila dopamine 2-like receptor: molecular characterization and identification of multiple alternatively spliced variants. Proc. Natl. Acad. Sci. USA *99*, 14554–14559.

Heigwer, F., Kerr, G., and Boutros, M. (2014). E-CRISP: fast CRISPR target site identification. Nat. Methods *11*, 122–123.

Henderson, J.E., Soderlund, D.M., and Knipple, D.C. (1993). Characterization of a putative gamma-aminobutyric acid (GABA) receptor beta subunit gene from Drosophila melanogaster. Biochem. Biophys. Res. Commun. *193*, 474–482.

Hendricks, J.C., Finn, S.M., Panckeri, K.A., Chavkin, J., Williams, J.A., Sehgal, A., and Pack, A.I. (2000). Rest in Drosophila is a sleep-like state. Neuron *25*, 129–138.

Herzog, E., Landry, M., Buhler, E., Bouali-Benazzouz, R., Legay, C., Henderson, C.E., Nagy, F., Dreyfus, P., Giros, B., and El Mestikawy, S. (2004a). Expression of vesicular glutamate transporters, VGLUT1 and VGLUT2, in cholinergic spinal motoneurons. Eur. J. Neurosci. *20*, 1752–1760.

Herzog, E., Gilchrist, J., Gras, C., Muzerelle, A., Ravassard, P., Giros, B., Gaspar, P., and El Mestikawy, S. (2004b). Localization of VGLUT3, the vesicular glutamate transporter type 3, in the rat brain. Neuroscience *123*, 983–1002.

Hewes, R.S., and Taghert, P.H. (2001). Neuropeptides and neuropeptide receptors in the Drosophila melanogaster genome. Genome Res. *11*, 1126–1142.

Hirasawa, H., Betensky, R.A., and Raviola, E. (2012). Corelease of dopamine and GABA by a retinal dopaminergic neuron. J. Neurosci. *32*, 13281–13291.

Hökfelt, T. (1991). Neuropeptides in perspective: the last ten years. Neuron *7*, 867–879.

Huang, J., Zhou, W., Dong, W., Watson, A.M., and Hong, Y. (2009). From the cover: directed, efficient, and versatile modifications of the Drosophila genome by genomic engineering. Proc. Natl. Acad. Sci. USA *106*, 8284–8289.

Hughes, J., Smith, T.W., Kosterlitz, H.W., Fothergill, L.A., Morgan, B.A., and Morris, H.R. (1975). Identification of two related pentapeptides from the brain with potent opiate agonist activity. Nature *258*, 577–580.

Hunt, R., and Taveau, M. (1906). On the physiological action of certain cholin derivatives and new methods for detecting cholin. BMJ *ii*, 1788–1789.

Ishimoto, H., and Kitamoto, T. (2010). The steroid molting hormone Ecdysone regulates sleep in adult Drosophila melanogaster. Genetics *185*, 269–281.

Itoh, N., Slemmon, J.R., Hawke, D.H., Williamson, R., Morita, E., Itakura, K., Roberts, E., Shively, J.E., Crawford, G.D., and Salvaterra, P.M. (1986). Cloning of Drosophila choline acetyltransferase cDNA. Proc. Natl. Acad. Sci. USA *83*, 4081–4085.

Jackson, F.R., Newby, L.M., and Kulkarni, S.J. (1990). Drosophila GABAergic systems: sequence and expression of glutamic acid decarboxylase. J. Neurochem. *54*, 1068–1078.

Jenett, A., Rubin, G.M., Ngo, T.T., Shepherd, D., Murphy, C., Dionne, H., Pfeiffer, B.D., Cavallaro, A., Hall, D., Jeter, J., et al. (2012). A GAL4-driver line resource for Drosophila neurobiology. Cell Rep. *2*, 991–1001.

Jonas, P., Bischofberger, J., and Sandkühler, J. (1998). Corelease of two fast neurotransmitters at a central synapse. Science *281*, 419–424.

Kao, Y.H., Lassová, L., Bar-Yehuda, T., Edwards, R.H., Sterling, P., and Vardi, N. (2004). Evidence that certain retinal bipolar cells use both glutamate and GABA. J. Comp. Neurol. *478*, 207–218.

Kasthuri, N., Hayworth, K.J., Berger, D.R., Schalek, R.L., Conchello, J.A., Knowles-Barley, S., Lee, D., Vázquez-Reina, A., Kaynig, V., Jones, T.R., et al. (2015). Saturated reconstruction of a volume of neocortex. Cell *162*, 648–661.

Kayser, M.S., Yue, Z., and Sehgal, A. (2014). A critical period of sleep for development of courtship circuitry and behavior in Drosophila. Science *344*, 269–274.

Kitamoto, T., Ikeda, K., and Salvaterra, P.M. (1992). Analysis of cis-regulatory elements in the 5′ flanking region of the Drosophila melanogaster choline acetyltransferase gene. J. Neurosci. *12*, 1628–1639.

Kong, E.C., Allouche, L., Chapot, P.A., Vranizan, K., Moore, M.S., Heberlein, U., and Wolf, F.W. (2010). Ethanol-regulated genes that contribute to ethanol sensitivity and rapid tolerance in Drosophila. Alcohol. Clin. Exp. Res. *34*, 302–316.

Kume, K., Kume, S., Park, S.K., Hirsh, J., and Jackson, F.R. (2005). Dopamine is a regulator of arousal in the fruit fly. J. Neurosci. *25*, 7377–7384.

Lerner, T.N., Ye, L., and Deisseroth, K. (2016). Communication in neural circuits: tools, opportunities, and challenges. Cell *164*, 1136–1150.

Liu, W.W., Liang, X.H., Li, Y.N., Gong, J.X., Yang, Z., Zhang, Y.H., Zhang, J.X., and Rao, Y. (2011). Social regulation of aggression mediated by pheromonal activation of Or65a olfactory receptor neurons in Drosophila. Nat. Neurosci. *14*, 896–902.

Liu, Q., Liu, S., Kodama, L., Driscoll, M.R., and Wu, M.N. (2012). Two dopaminergic neurons signal to the dorsal fan-shaped body to promote wakefulness in Drosophila. Curr. Biol. *22*, 2114–2123.

Loewi, O. (1921). Über humorale Übertragbarkeit der Herznervenwirkung. Pflügers Arch. ges Physiol *189*, 239–242.

Lu, J., Jhou, T.C., and Saper, C.B. (2006). Identification of wake-active dopaminergic neurons in the ventral periaqueductal gray matter. J. Neurosci. *26*, 193–202.

Luan, H., Peabody, N.C., Vinson, C.R., and White, B.H. (2006). Refined spatial manipulation of neuronal function by combinatorial restriction of transgene expression. Neuron *52*, 425–436.

Lundberg, J.M. (1996). Pharmacology of cotransmission in the autonomic nervous system: integrative aspects on amines, neuropeptides, adenosine triphosphate, amino acids and nitric oxide. Pharmacol. Rev. *48*, 113–178.

Luo, L., Callaway, E.M., and Svoboda, K. (2018). Genetic dissection of neural circuits: a decade of progress. Neuron *98*, 256–281.

Ma, Z., Stork, T., Bergles, D.E., and Freeman, M.R. (2016). Neuromodulators signal through astrocytes to alter neural circuit activity and behaviour. Nature *539*, 428–432.

Mao, Z., and Davis, R.L. (2009). Eight different types of dopaminergic neurons innervate the Drosophila mushroom body neuropil: anatomical and physiological heterogeneity. Front. Neural Circuits *3*, 5.

Mendez, J.A., Bourque, M.J., Dal Bo, G., Bourdeau, M.L., Danik, M., Williams, S., Lacaille, J.-C., and Trudeau, L.-E. (2008). Developmental and target-dependent regulation of vesicular glutamate transporter expression by dopamine neurons. J. Neurosci. *28*, 6309–6318.

Mezler, M., Müller, T., and Raming, K. (2001). Cloning and functional expression of GABA(B) receptors from Drosophila. Eur. J. Neurosci. *13*, 477–486.

Monastirioti, M., Linn, C.E., Jr., and White, K. (1996). Characterization of Drosophila tyramine β-hydroxylase gene and isolation of mutant flies lacking octopamine. J. Neurosci. *16*, 3900–3911.

Montagu, K.A. (1957). Catechol compounds in rat tissues and in brains of different animals. Nature *180*, 244–245.

Morgan, J.L., Berger, D.R., Wetzel, A.W., and Lichtman, J.W. (2016). The fuzzy logic of network connectivity in mouse visual thalamus. Cell *165*, 192–206.

Münster-Wandowski, A., Zander, J.F., Richter, K., and Ahnert-Hilger, G. (2016). Co-existence of functionally different vesicular neurotransmitter transporters. Front. Synaptic Neurosci. *8*, 4.

Nall, A.H., Shakhmantsir, I., Cichewicz, K., Birman, S., Hirsh, J., and Sehgal, A. (2016). Caffeine promotes wakefulness via dopamine signaling in Drosophila. Sci. Rep. *6*, 20938.

Nässel, D.R., and Winther, A.M.E. (2010). Drosophila neuropeptides in regulation of physiology and behavior. Prog. Neurobiol. *92*, 42–104.

Neckameyer, W.S., and Quinn, W.G. (1989). Isolation and characterization of the gene for Drosophila tyrosine hydroxylase. Neuron *2*, 1167–1175.

Neckameyer, W.S., and White, K. (1992). A single locus encodes both phenylalanine-hydroxylase and tryptophan-hydroxylase activities in Drosophila. J. Biol. Chem. *267*, 4199–4206.

Ng, F.S., Tangredi, M.M., and Jackson, F.R. (2011). Glial cells physiologically modulate clock neurons and circadian behavior in a calcium-dependent manner. Curr. Biol. *21*, 625–634.

Ng, F.S., Sengupta, S., Huang, Y., Yu, A.M., You, S., Roberts, M.A., Iyer, L.K., Yang, Y., and Jackson, F.R. (2016). TRAP-seq profiling and RNAi-based genetic screens identify conserved glial genes required for adult Drosophila behavior. Front. Mol. Neurosci. *9*, 146.

Nicoll, R.A., and Malenka, R.C. (1998). A tale of two transmitters. Science *281*, 360–361.

Nusbaum, M.P., Blitz, D.M., and Marder, E. (2017). Functional consequences of neuropeptide and small-molecule co-transmission. Nat. Rev. Neurosci. *18*, 389–403.

Oh, S.W., Harris, J.A., Ng, L., Winslow, B., Cain, N., Mihalas, S., Wang, Q., Lau, C., Kuan, L., Henry, A.M., et al. (2014a). A mesoscale connectome of the mouse brain. Nature *508*, 207–214.

Oh, Y., Yoon, S.E., Zhang, Q., Chae, H.S., Daubnerová, I., Shafer, O.T., Choe, J., and Kim, Y.J. (2014b). A homeostatic sleep-stabilizing pathway in *Drosophila* composed of the sex peptide receptor and its ligand, the myoinhibitory peptide. PLoS Biol. *12*, e1001974.

Oliver, G., and Schäfer, E.A. (1895). The physiological effects of extracts of the suprarenal capsules. J. Physiol. *18*, 230–276.

Ottem, E.N., Godwin, J.G., Krishnan, S., and Petersen, S.L. (2004). Dual-phenotype GABA/glutamate neurons in adult preoptic area: sexual dimorphism and function. J. Neurosci. *24*, 8097–8105.

Park, S., Sonn, J.Y., Oh, Y., Lim, C., and Choe, J. (2014). SIFamide and SIFamide receptor defines a novel neuropeptide signaling to promote sleep in Drosophila. Mol. Cells *37*, 295–301.

Pédelacq, J.D., Cabantous, S., Tran, T., Terwilliger, T.C., and Waldo, G.S. (2006). Engineering and characterization of a superfolder green fluorescent protein. Nat. Biotechnol. *24*, 79–88.

Pfeiffenberger, C., and Allada, R. (2012). Cul3 and the BTB adaptor insomniac are key regulators of sleep homeostasis and a dopamine arousal pathway in Drosophila. PLoS Genet. *8*, e1003003.

Pfeiffer, B.D., Ngo, T.T.B., Hibbard, K.L., Murphy, C., Jenett, A., Truman, J.W., and Rubin, G.M. (2010). Refinement of tools for targeted gene expression in Drosophila. Genetics *186*, 735–755.

Pimentel, D., Donlea, J.M., Talbot, C.B., Song, S.M., Thurston, A.J.F., and Miesenböck, G. (2016). Operation of a homeostatic sleep switch. Nature *536*, 333–337.

Pörzgen, P., Park, S.K., Hirsh, J., Sonders, M.S., and Amara, S.G. (2001). The antidepressant-sensitive dopamine transporter in Drosophila melanogaster: a primordial carrier for catecholamines. Mol. Pharmacol. *59*, 83–95.

Qian, Y., Cao, Y., Deng, B., Yang, G., Li, J., Xu, R., Zhang, D., Huang, J., and Rao, Y. (2017). Sleep homeostasis regulated by 5HT2b receptor in a small subset of neurons in the dorsal fan-shaped body of Drosophila. eLife *6*, e26519.

Qu, W.M., Xu, X.H., Yan, M.M., Wang, Y.Q., Urade, Y., and Huang, Z.L. (2010). Essential role of dopamine D2 receptor in the maintenance of wakefulness, but not in homeostatic regulation of sleep, in mice. J. Neurosci. *30*, 4382–4389.

Ran, F.A., Hsu, P.D.P., Wright, J., Agarwala, V., Scott, D.A., and Zhang, F. (2013). Genome engineering using the CRISPR-Cas9 system. Nat. Protoc. *8*, 2281–2308.

Rapport, M.M., Green, A.A., and Page, I.H. (1948). Serum vasoconstrictor, serotonin; isolation and characterization. J. Biol. Chem. *176*, 1243–1251.

Ren, X., Sun, J., Housden, B.E., Hu, Y., Roesel, C., Lin, S., Liu, L.-P., Yang, Z., Mao, D., Sun, L., et al. (2013). Optimized gene editing technology for Drosophila melanogaster using germ line-specific Cas9. Proc. Natl. Acad. Sci. USA *110*, 19012–19017.

Roberts, E., and Frankel, S. (1950). γ-Aminobutyric acid in brain: its formation from glutamic acid. J. Biol. Chem. *187*, 55–63.

Roeder, T. (2005). Tyramine and octopamine: ruling behavior and metabolism. Annu. Rev. Entomol. *50*, 447–477.

Rong, Y.S., and Golic, K.G. (2000). Gene targeting by homologous recombination in Drosophila. Science *288*, 2013–2018.

Rong, Y.S., and Golic, K.G. (2001). A targeted gene knockout in Drosophila. Genetics *157*, 1307–1312.

Schäfer, M.K., Varoqui, H., Defamie, N., Weihe, E., and Erickson, J.D. (2002). Molecular cloning and functional identification of mouse vesicular glutamate transporter 3 and its expression in subsets of novel excitatory neurons. J. Biol. Chem. *277*, 50734–50748.

Seidner, G., Robinson, J.E., Wu, M., Worden, K., Masek, P., Roberts, S.W., Keene, A.C., and Joiner, W.J. (2015). Identification of neurons with a privileged role in sleep homeostasis in Drosophila melanogaster. Curr. Biol. *25*, 2928–2938.

Selcho, M., Millán, C., Palacios-Muñoz, A., Ruf, F., Ubillo, L., Chen, J., Bergmann, G., Ito, C., Silva, V., Wegener, C., and Ewer, J. (2017). Central and peripheral clocks are coupled by a neuropeptide pathway in Drosophila. Nat. Commun. *8*, 15563.

Seugnet, L., Suzuki, Y., Merlin, G., Gottschalk, L., Duntley, S.P., and Shaw, P.J. (2011). Notch signaling modulates sleep homeostasis and learning after sleep deprivation in Drosophila. Curr. Biol. *21*, 835–840.

Shaw, P.J., Cirelli, C., Greenspan, R.J., and Tononi, G. (2000). Correlates of sleep and waking in Drosophila melanogaster. Science *287*, 1834–1837.

Sitaraman, D., Aso, Y., Rubin, G.M., and Nitabach, M.N. (2015). Control of sleep by dopaminergic inputs to the Drosophila mushroom body. Front. Neural Circuits *9*, 73.

Sporns, O., Tononi, G., and Kötter, R. (2005). The human connectome: a structural description of the human brain. PLoS Comput. Biol. *1*, 0245–0251.

Suh, J., and Jackson, F.R. (2007). Drosophila ebony activity is required in glia for the circadian regulation of locomotor activity. Neuron *55*, 435–447.

Takamine, J. (1901). Adrenalin, the active principle of the suprarenal glands, and its mode of preparation. Am. J. Pharm. *73*, 523–531.

Takamine, J. (1902). The isolation of the active principle of the suprarenal gland. J. Physiol. *27*, 29–30.

Tecuapetla, F., Patel, J.C., Xenias, H., English, D., Tadros, I., Shah, F., Berlin, J., Deisseroth, K., Rice, M.E., Tepper, J.M., and Koos, T. (2010). Glutamatergic signaling by mesolimbic dopamine neurons in the nucleus accumbens. J. Neurosci. *30*, 7105–7110.

Terhzaz, S., Rosay, P., Goodwin, S.F., and Veenstra, J.A. (2007). The neuropeptide SIFamide modulates sexual behavior in Drosophila. Biochem. Biophys. Res. Commun *352*, 305–310.

Thum, A.S., Knapek, S., Rister, J., Dierichs-Schmitt, E., Heisenberg, M., and Tanimoto, H. (2006). Differential potencies of effector genes in adult Drosophila. J. Comp. Neurol. *498*, 194–203.

Ting, C.Y., Gu, S., Guttikonda, S., Lin, T.Y., White, B.H., and Lee, C.H. (2011). Focusing transgene expression in Drosophila by coupling Gal4 with a novel split-LexA expression system. Genetics *188*, 229–233.

Trudeau, L.E. (2004). Glutamate co-transmission as an emerging concept in monoamine neuron function. J. Psychiatry Neurosci. *29*, 296–310.

Udenfriend, S. (1950). Identification of gamma-aminobutyric acid in brain by the isotope derivative method. J. Biol. Chem. *187*, 65–69.

Ueno, T., Tomita, J., Tanimoto, H., Endo, K., Ito, K., Kume, S., and Kume, K. (2012). Identification of a dopamine pathway that regulates sleep and arousal in Drosophila. Nat. Neurosci. *15*, 1516–1523.

Von Euler, U.S. (1946). A specific sympathomimetic ergone in adrenergic nerve fibers (sympathin) and its relations to adrenaline and nor-adrenaline. Acta Physiol. Scand. *12*, 73–97.

Von Euler, U.S., and Gaddum, J.H. (1931). An unidentified depressor substance in certain tissue extracts. J. Physiol. *72*, 74–87.

Venken, K.J.T., Schulze, K.L., Haelterman, N.A., Pan, H., He, Y., Evans-Holm, M., Carlson, J.W., Levis, R.W., Spradling, A.C., Hoskins, R.A., and Bellen, H.J. (2011). MiMIC: a highly versatile transposon insertion resource for engineering Drosophila melanogaster genes. Nat. Methods *8*, 737–743.

Watabe-Uchida, M., Zhu, L., Ogawa, S.K., Vamanrao, A., and Uchida, N. (2012). Whole-brain mapping of direct inputs to midbrain dopamine neurons. Neuron *74*, 858–873.

White, J.G., Southgate, E., Thomson, J.N., and Brenner, S. (1986). The structure of the nervous system of the nematode Caenorhabditis elegans. Philos. Trans. R. Soc. Lond. B Biol. Sci. *314*, 1–340.

Wisor, J.P., Nishino, S., Sora, I., Uhl, G.H., Mignot, E., and Edgar, D.M. (2001). Dopaminergic role in stimulant-induced wakefulness. J. Neurosci. *21*, 1787–1794.

Wu, Q., and Palmiter, R.D. (2011). GABAergic signaling by AgRP neurons prevents anorexia via a melanocortin-independent mechanism. Eur. J. Pharmacol. *660*, 21–27.

Yamazaki, D., Horiuchi, J., Ueno, K., Ueno, T., Saeki, S., Matsuno, M., Naganos, S., Miyashita, T., Hirano, Y., Nishikawa, H., et al. (2014). Glial dysfunction causes age-related memory impairment in Drosophila. Neuron *84*, 753–763.

Yuan, Q., Joiner, W.J., and Sehgal, A. (2006). A sleep-promoting role for the *Drosophila* serotonin receptor 1A. Curr. Biol. *16*, 1051–1062.

Zander, J.F., Münster-Wandowski, A., Brunk, I., Pahner, I., Gómez-Lira, G., Heinemann, U., Gutiérrez, R., Laube, G., and Ahnert-Hilger, G. (2010). Synaptic and vesicular coexistence of VGLUT and VGAT in selected excitatory and inhibitory synapses. J. Neurosci. *30*, 7634–7645.

Zhang, S., Qi, J., Li, X., Wang, H.L., Britt, J.P., Hoffman, A.F., Bonci, A., Lupica, C.R., and Morales, M. (2015). Dopaminergic and glutamatergic microdomains in a subset of rodent mesoaccumbens axons. Nat. Neurosci. *18*, 386–392.

Zhang, S.L., Yue, Z., Arnold, D.M., Artiushin, G., and Sehgal, A. (2018). A circadian clock in the blood-brain barrier regulates xenobiotic efflux. Cell *173*, 130–139.e10.

Zheng, Z., Lauritzen, J.S., Perlman, E., Robinson, C.G., Nichols, M., Milkie, D., Torrens, O., Price, J., Fisher, C.B., Sharifi, N., et al. (2018). A complete electron microscopy volume of the brain of adult Drosophila melanogaster. Cell *174*, 730–743.e22.

Zhou, C., Rao, Y., and Rao, Y. (2008). A subset of octopaminergic neurons are important for Drosophila aggression. Nat. Neurosci. *11*, 1059–1067.

Zhou, C., Huang, H., Kim, S.M., Lin, H., Meng, X., Han, K.A., Chiang, A.S., Wang, J.W., Jiao, R., and Rao, Y. (2012). Molecular genetic analysis of sexual rejection: roles of octopamine and its receptor OAMB in Drosophila courtship conditioning. J. Neurosci. *32*, 14281–14287.

STAR★METHODS

KEY RESOURCES TABLE

REAGENT or RESOURCE	SOURCE	IDENTIFIER
Antibodies		
Mouse anti-Bruchpilot antibody (nc82)	Developmental Studies Hybridoma Bank	RRID: AB_2314866
Rat anti-elav	Developmental Studies Hybridoma Bank	RRID: AB_528218
Mouse anti-Repo	Developmental Studies Hybridoma Bank	RRID: AB_528448
Rabbit anti-TH	Novus Biologicals	NOVUS NB300-109; RRID: AB_10077691
Chicken anti-GFP antibody	Abcam	Cat# 13970, RRID: AB_300798
Goat anti-chicken, Alexa488	Thermo Fisher Scientific	Cat#A-11039; RRID: AB_2534096
Goat anti-rabbit, Alex546	Thermo Fisher Scientific	Cat# A11035, RRID: AB_253409
Goat anti-mouse, Alexa633	Thermo Fisher Scientific	Cat#A-21050; RRID: AB_2535718
Rabbit anti-Dilp2	Gong Lab, Zhejiang University	N/A
Mouse anti-PDF	Developmental Studies Hybridoma Bank	PDF C7; RRID: AB_760350
Rabbit anti-SIFamide	Veenstra Lab, University of Bordeaux	N/A
Chemicals, Peptides, and Recombinant Proteins		
Normal goat serum	Sigma	Cat# G9023
L-DOPA	Sigma	Cat#D9628
Paraformaldehyde (PFA)	Electron Microscopy Sciences	Cat#15713
Focus Clear	Cell Explorer Labs	Cat# FC-101
Experimental Models: Organisms/Strains		
Drosophila: vas-Cas9	Ni Lab, Tsinghua University	N/A
Drosophila: UAS-Stinger::GFP	Dickson, Janelia Research Campus	N/A
Drosophila: LexAop-tdTomato	Dickson lab, Janelia Research Campus	N/A
Drosophila: 13XLexAop2-IVS-myr::GFP (attp5)	Rubin Lab, Janelia Research Campus	N/A
Drosophila: 13XLexAop2-IVS-myr::GFP (attp2)	Rubin Lab, Janelia Research Campus	N/A
Drosophila: UAS-LexA DBD	Lee Lab, NIH	N/A
Drosophila: TβH^{nM18}	Wu Lab, University of Iowa	N/A
Drosophila: TH-Gal4	Hirsh Lab, University of Virginia	N/A
Drosophila: SIFa-Gal4	Veenstra Lab, University of Bordeaux	N/A
Drosophila: c739	Griffith Lab, Brandeis University	N/A
Drosophila: c309	Griffith Lab, Brandeis University	N/A
Drosophila: NP1131	Dubnau Lab, Cold Spring Harbor Laboratory	N/A
Drosophila: c305a	Dubnau Lab, Cold Spring Harbor Laboratory	N/A
Drosophila: Pdf-Gal4	Allada Lab, Northwestern University	N/A
Drosophila: NP6293-Gal4	Ito Lab, University of Tokyo	N/A
Drosophila: NP2276-Gal4	Ito Lab, University of Tokyo	N/A
Drosophila: NP2222-Gal4	Ito Lab, University of Tokyo	N/A
Drosophila: NP1243-Gal4	Ito Lab, University of Tokyo	N/A
Drosophila: NP6520-Gal4	Ito Lab, University of Tokyo	N/A
Drosophila: NP3233-Gal4	Ito Lab, University of Tokyo	N/A
Drosophila: UAS-dTrpA1	Garrity Lab, Brandeis University	N/A
Drosophila: y1v1P{nos-phiC31\int.NLS}X; {CarryP}attP40	Bloomington Stock Center	#25709
Drosophila: 23E10-Gal4	Bloomington Stock Center	#49032
Drosophila: c767	Bloomington Stock Center	#30848
Drosophila: 50Y	Bloomington Stock Center	#30820

(*Continued on next page*)

Continued

REAGENT or RESOURCE	SOURCE	IDENTIFIER
Drosophila: dilp2-Gal4	Bloomington Stock Center	#37516
Drosophila: DH44-Gal4	Bloomington Stock Center	#51987
Drosophila: UAS-mCD8-GFP	Bloomington Stock Center	#5137
Drosophila: y^1 w^{67c23} P{Crey}1b; sna^{Sco}/CyO	Bloomington Stock Center	#766
Drosophila: y^1 w^{67c23} P{Crey}1b; D/TM3,Sb^1*	Bloomington Stock Center	#851
Drosophila: y^1 w^{67c23}; sna^{Sco}/CyO, P{Crew}DH1	Bloomington Stock Center	#1092
Drosophila: y^1 w; P{UAS-NaChBac}2*	Bloomington Stock Center	#9469
Drosophila: w; P{UAS-Hsap\KCNJ2.EGFP}7*	Bloomington Stock Center	#6595
Drosophila: w^{1118}; P{8XLexAop2-FLPL}attP2	Bloomington Stock Center	#55819
Drosophila: UAS-FRT-stop-FRT-mCD8GFP	Bloomington Stock Center	#30032
Drosophila: UAS-Octβ2R (attp40)	Rao Lab, Peking University, this paper	N/A
Drosophila: UAS-Dop2R (attp40)	Rao Lab, Peking University, this paper	N/A
Drosophila: other KO and KI flies	Rao Lab, Peking University, this paper	N/A
Recombinant DNA		
pACU2	Jan Lab, University of California, San Francisco, Han et al., 2011	N/A
pGE-attB	Huang et al., 2009	N/A
U6b-sgRNA-short	Ni Lab, Tsinghua University, Ren et al., 2013	N/A
pEASY-RFP	Gao Lab, Tsinghua University	N/A
pBluescript SK (+)	Xi Lab, National Institute of Biological Sciences, Beijing	N/A
pBPnlsLexA::GADflUw	Pfeiffer et al., 2010	Addgene: #26232
pBPp65ADZpUw	Pfeiffer et al., 2010	Addgene: #26234
pBPZpGAL4DBDUw	Pfeiffer et al., 2010	Addgene: #26233
pBPGUw	Pfeiffer et al., 2010	Addgene: #17575
pBPLexA::p65Uw	Pfeiffer et al., 2010	Addgene: #26231
pBS-KS-attB1-2-GT-SA-Flpo-SV40	Venken et al., 2011	Drosophila Genomics Resource Center: #1326
sfGFP-pBAD	Pédelacq et al., 2006	Addgene: #54519
pBSK-attP-3P3-RFP-loxP	Rao Lab, Peking University, this paper	N/A
pBSK-attB-loxP-myc-T2A-Gal4-GMR-miniwhite	Rao Lab, Peking University, this paper	N/A
pBSK-attB-loxP-V5-T2A-nlsLexA::GAD-GMR-miniwhite	Rao Lab, Peking University, this paper	N/A
pBSK-attB-loxP-V5-T2A-LexA::p65-GMR-miniwhite	Rao Lab, Peking University, this paper	N/A
pBSK-attB-loxP-myc-T2A-Flpo-GMR-miniwhite	Rao Lab, Peking University, this paper	N/A
pBSK-attB-loxP-T2A-p65ADzp-GMR-miniwhite	Rao Lab, Peking University, this paper	N/A
pBSK-attB-loxP-sfGFP-GMR-miniwhite	Rao Lab, Peking University, this paper	N/A
Software and Algorithms		
MATLAB	MathWorks, Natick, MA	https://www.mathworks.com/products/matlab.html
Prism 5	GraphPad	https://www.graphpad.com/
Imaris	Bitplane	http://www.bitplane.com/imaris/imaris

CONTACT FOR REAGENT AND RESOURCE SHARING

Further information and requests for resources and reagents should be directed to and will be fulfilled by the Lead Contact, Yi Rao (yrao@pku.edu.cn).

EXPERIMENTAL MODEL AND SUBJECT DETAILS

Fly Lines and Rearing Conditions

Flies were reared on standard corn meal at 25°C, 60% humidity, 12 h light:12 h dark (LD) cycle. For flies used in behavior assays, we backcrossed all of them into our isogenized Canton S background for 7 generations. For the *UAS-dTrpA1* experiment, flies were reared at 18°C. *vas-Cas9* was a gift from Dr. J. Ni (Tsinghua University, Beijing). *UAS-Stinger::GFP* and *LexAop-tdTomato* were gifts from Dr. B. Dickson (Janelia Research Campus, HHMI). *UAS-LexADBD* was a gift from Dr. C. H. Lee (NIH). $T\beta H^{nM18}$ null mutant was a gift from Chun-Fang Wu (University of Iowa). *UAS-dTrpA1* was a gift from Dr. P. Garrity (Brandeis University). *TH-Gal4* was a gift from Dr. J. Hirsh (University of Virginia). *SIFa-Gal4* was a gift from Dr. J. Veenstra (University of Bordeaux). *c739* and *c309* were gifts from Dr. L. Griffith (Brandeis University). *NP1131* and *c305a* were gifts from Dr. J. Dubnau (Cold Spring Harbor Laboratory). *Pdf-Gal4* was a gift from Dr. R. Allada (Northwestern University). nos-phiC31, *23E10* (BL#49032), *c767* (BL#30848), *50Y* (BL#30820), *dilp2* (BL#37516), *DH44* (BL#51987), *UAS-mCD8-GFP* (BL#5137), *hs-Cre* on X or second chromosome (i.e., BL#766, BL#851 and BL#1092), *UAS-NachBac* (BL#9469), *UAS-Kir2.1* (BL#6595) were obtained from the Bloomington Stock Center.

METHOD DETAILS

Gene Selection

The list of genes was acquired from Flybase and previous reports. Genes coding transmitter synthetase, neuropeptides, transmitter transporters, transmitter receptors and GPCRs were selected whereas GPCRs used in olfaction, taste, and vision as well as adhesion GPCRs were excluded. Some genes were newly annotated in the databases after our work began. The final list of the 193 genes is shown in Table S2.

Molecular Biology

All the KO lines were generated through homologous recombination in *Drosophila* embryos with the CRISPR/Cas9 system, though we also generated an additional set of KO lines for DRs with the ends-in and ends-out methods (Rong and Golic, 2000, 2001).

To generate the targeting vector, a plasmid containing attP-3P3-RFP-loxP cassette was modified from pEASY-RFP (a gift from Guanjun Gao, Tsinghua University, Beijing) by adding the loxP sequence and the 53 bp minimal attP sequence (Huang et al., 2009). The targeting vector arms were generated by cloning the 5′ARM and 3′ARM of a gene into the KpnI and SacII digested pBSK+ plasmid through Gibson assembly (Gibson et al., 2009), and the arm sequences were confirmed by restriction enzyme digestion and sequencing. attP-3P3-RFP-loxP cassette was inserted between the two arms by restriction enzyme digestion and ligation.

The sgRNAs were designed using online sgRNA design web E-CRISP (http://www.e-crisp.org/E-CRISP/) (Heigwer et al., 2014), and the sgRNA constructs were generated as described previously (Ren et al., 2013). For each gene, two sgRNA constructs were generated, with one after the 5′arm ending site and one before the 3′ arm starting site. KI flies were generated through phiC31 mediated attB/attP recombination, and the miniwhite gene was used as a selection marker. The pBSK-attB-GMR miniwhite vector was generated by inserting the attB-GMR miniwhite cassette from pGE-attB (Huang et al., 2009) into the KpnI and SacII digested pBSK+ plasmid. Coding sequences for 2xMyc-T2A-Gal4, V5-T2A-LexA, T2A-zp-p65AD, 2xMyc-T2A-Flp and sfGFP were inserted into pBSK-attB-GMR miniwhite to generate pBSK-attB-2xMyc-T2A-Gal4, pBSK-attB-V5-T2A-LexA, pBSK-attB-T2A-zp-p65AD, pBSK-attB-2xMyc-T2A-Flp, and pBSK-attB- sfGFP KI backbone vectors. To generate the KI vector for each gene, genomic region from the ending site of the 5′ arm to stop codon was cloned into the KI backbone vectors though Gibson assembly. For genes with different isoforms, the sequence from the shorter isoform's stop codon to the starting site of the 3′ arm was cloned and inserted after Gal4/LexA by Gibson assembly into the SpeI digested KI plasmid.

The *UAS-Octβ2R* and *UAS-Dop2R* DNA construct were generated by cloning the *Octβ2R* and *Dop2R* open reading frames amplified from fly head cDNA into the pACU2 vector (a gift from the Jan Lab at UCSF) (Han et al., 2011).

Generation of KO, KI and Transgenic Lines

To generate KO lines, a plasmid mixture with the targeting vector and two sgRNAs were diluted in sterile water at a final concentration of 500 ng/μl for targeting vector and 250 ng/μl for each sgRNA plasmid. Plasmids were injected into *vas-cas9* embryos. F1 flies with RFP positive eyes were selected as KO candidates and verified by polymerase chain reaction (PCR) followed by sequencing. To generated KI lines, the nos-phiC31 virgin females were first crossed with the KO males, then the KI vectors (300∼500ng/μl) were injected into the embryos from these females. F1 flies with red eyes were selected as KI candidates and verified by PCR.

The resulting KI lines were balanced before being crossed to *hs-Cre* flies to remove all unnecessary DNA sequences including the 3P3-RFP, GMR miniwhite and construct backbones.

UAS-Octβ2R and *UAS-Dop2R* DNA constructs were injected and integrated into the attP40 site on the second chromosome through phiC31 mediated gene integration. Transgenic flies were obtained and confirmed by PCR.

Behavioral Assays

For sleep analysis, virgin females of 4 to 6 days were individually loaded into 5x65mm glass tubes with food. Before sleep measurement, flies were entrained to a 12 h light:12 h dark cycle at 25°C for at least two days. Locomotion was recorded by a camera with

704x576 resolution. In order to clearly videotape fly locomotion in the dark period, we used infrared LED light. Videos were taken at 5 frames per second. 1 frame per second was extracted for fly tracing. The tracing was analyzed with an in-house software (Qian et al., 2017). Sleep was defined by the traditional 5 min or longer immobility (Hendricks et al., 2000; Shaw et al., 2000). DAM-based method to measure sleep used the same video recorded data. By defining a virtual beam in the center of the recording tubes, midline crossings were counted with a software based on MATLAB.

For neuronal activation experiments by *UAS-dTrpA1*, flies were reared at 18°C. Virgin females were selected and maintained at 18°C for 8 to 10 days before being recorded at 23°C for 3 days as the baseline and at 28°C for 1 day activation. Sleep bout duration and bout number were calculated as the mean bout duration and mean bout number respectively.

Sleep deprivation was performed as previously described (Qian et al., 2017). Briefly, a plastic holder with recording tubes was fixed into a holding box. The holding box was rotated and bumped onto plastic stoppers under the control of a motor driver. The motor driver was randomly activated every 3 min for 12 h during the night. The recovery rate was calculated as (sleep after SD-sleep before SD)/sleep loss by SD. Female flies were used in the sleep deprivation assay.

Aggression was analyzed as that described in our previous studies (Zhou et al., 2008; Liu et al., 2011). Two isolated male flies of the same genotype were introduced to the aggression chamber at age 5 to 7 days. Latency and frequency were used to measure the aggression level.

L-DOPA Feeding

Virgin females of 4 to 6 days old were individually loaded into 5x65mm glass tubes with food containing 2% agar and 5% sucrose. Flies were allowed to habituate for 3 days at 25°C, 12 h light: 12 h dark cycle as the baseline (basal sleep). Flies were then transferred into food containing 4 mg/ml L-DOPA. Flies were presented with L-DOPA for 20 h before sleep recording. Sleep on the following day (still on L-DOPA food) was analyzed. Sleep loss ratio was calculated as (basal sleep-sleep on L-DOPA food)/ basal sleep.

Immunohistochemistry and Confocal Imaging

For all immunostainings, 6 to 10 days old adult flies were anesthetized and dissected in ice-cold phosphate buffered saline (PBS). Whole-mount brains were fixed in 4% paraformaldehyde (wt/vol) for 2 h on ice, washed three times in 0.03% PBST (PBS containing 0.03% Triton X-100 (vol/vol)) for 10 min at room temperature. Brains were subject to 10% normal goat serum (diluted in 2% PBST) for 12 h blocking and penetration at 4°C, before incubation with the primary antibody (diluted in 1% normal goat serum in 0.25% PBST) for 24 h at 4°C. Samples were washed in 3% sodium chloride in 1% PBST for three times for 15 min before incubation with the secondary antibody (diluted in 1% normal goat serum in 0.25% PBST) for 24 h in darkness at 4°C. Samples were washed three times for 15 min, before being mounted on slices in Focus Clear (Cell Explorer Labs, FC-101), and visualized on a Zeiss LSM 710 confocal microscope. Images were processed by Imaris and ZEN blue softwares. The following primary antibodies were used: chicken anti-GFP (1:1000; Abcam), mouse anti-nc82 (1:50; DSHB), mouse anti-PDF (1:200; DSHB), rabbit anti-TH (1:500; Novus Biologicals). Rabbit anti-Dilp2 (1:1000) was a gift from Dr. Z. F. Gong (Zhejiang University). Rabbit anti-SIFamide (1:1000) was a gift from Dr. J. Veenstra (University of Bordeaux) (Terhzaz et al., 2007). The following secondary antibodies were used: Alexa Fluor goat anti-chicken 488 (1:1000; Invitrogen), Alexa Fluor goat anti-mouse 633 (1:200; Invitrogen) and Alexa Fluor goat anti-rabbit 546 (1:500; Invitrogen).

QUANTIFICATION AND STATISTICAL ANALYSIS

The Mann Whitney test was used to compare two columns in Figures S5G and S5H, and to compare the sleep level of KO lines with w1118 in Table S3. The Kruskal-Wallis ANOVA test, followed by Dunns post test, was used to compare multiple columns of data. All statistical analyses were carried out with Prism 5 (GraphPad Software). The sample sizes and statistical tests used for each experiment are stated in the figures or figure legends.